



# Research

Fatigue Evaluation of the  
Deck Truss of Bridge 9340

## Technical Report Documentation Page

1. Report No. MN/RC – 2001-10	2.	3. Recipients Accession No.	
4. Title and Subtitle FATIGUE EVALUATION OF THE DECK TRUSS OF BRIDGE 9340		5. Report Date March 2001	
		6.	
7. Author(s) Heather M. O’Connell, Robert J. Dexter, P.E. and Paul M. Bergson, P.E.		8. Performing Organization Report No.	
9. Performing Organization Name and Address Department of Civil Engineering University of Minnesota 500 Pillsbury Drive SE Minneapolis, MN 55455-0116		10. Project/Task/Work Unit No.	
		11. Contract (C) or Grant (G) No. c) 74708 wo) 124	
12. Sponsoring Organization Name and Address Minnesota Department of Transportation 395 John Ireland Boulevard Mail Stop 330 St. Paul, Minnesota 55155		13. Type of Report and Period Covered Final Report 2000-2001	
		14. Sponsoring Agency Code	
15. Supplementary Notes			
16. Abstract (Limit: 200 words)  <p>This research project resulted in a new, accurate way to assess fatigue cracking on Bridge 9340 on I-35, which crosses the Mississippi River near downtown Minneapolis.</p> <p>The research involved installation on both the main trusses and the floor truss to measure the live-load stress ranges. Researchers monitored the strain gages while trucks with known axle weights crossed the bridge under normal traffic. Researchers then developed two-and three-dimensional finite-element models of the bridge, and used the models to calculate the stress ranges throughout the deck truss.</p> <p>The bridge’s deck truss has not experienced fatigue cracking, but it has many poor fatigue details on the main truss and floor truss system. The research helped determine that the fatigue cracking of the deck truss is not likely, which means that the bridge should not have any problems with fatigue cracking in the foreseeable future.</p> <p>As a result, Mn/DOT does not need to prematurely replace this bridge because of fatigue cracking, avoiding the high costs associated with such a large project.</p> <p>The research also has implications for other bridges. The project verified that the use of strain gages at key locations combined with detailed analysis help predict the bridge’s behavior. In addition, the instrumentation plan can be used in other similar bridges.</p>			
17. Document Analysis/Descriptors Bridge Truss Fatigue Bridge Truss Maintenance Steel Transportation Structures		18. Availability Statement No restrictions. Document available from: National Technical Information Services, Springfield, Virginia 22161	
19. Security Class (this report)  Unclassified	20. Security Class (this page)  Unclassified	21. No. of Pages  91	22. Price

# **FATIGUE EVALUATION OF THE DECK TRUSS OF BRIDGE 9340**

## **Final Report**

*Prepared by:*

Heather M. O'Connell  
Robert J. Dexter, P.E.  
Paul Bergson, P.E.

University of Minnesota  
Department of Civil Engineering  
500 Pillsbury Drive S.E.  
Minneapolis, MN 55455-0116

**March 2001**

*Published by:*

Minnesota Department of Transportation  
Office of Research Services  
Mail Stop 330  
395 John Ireland Boulevard  
St. Paul, MN 55155

This report presents the results of research conducted by the authors and does not necessarily reflect the views of the Minnesota Department of Transportation. This report does not constitute a standard or specification.

## **ACKNOWLEDGEMENTS**

The authors appreciate the support of Minnesota Department of Transportation and the Administrative support of the Center for Transportation Studies at the University of Minnesota. The authors are grateful for the guidance of Donald Flemming, former State Bridge Engineer, and Gary Peterson. The logistical support of the Metro Division, particularly Mark Pribula, is also appreciated.

# TABLE OF CONTENTS

Chapter 1	INTRODUCTION .....	1
	Problem Statement .....	1
	Objective of Research .....	5
	Scope of Report .....	5
Chapter 2	BACKGROUND .....	7
	Fatigue Resistance .....	7
	Structural Redundancy .....	10
	Calculated and Actual Response .....	11
	Fatigue Evaluation Procedures .....	16
	Guide Specifications for the Fatigue Evaluation of Existing Bridges .....	18
	Effective Stress Range .....	19
	Reliability Factor .....	20
	Stress Cycles Per Truck Passage .....	21
	Fatigue Curve Constants .....	21
	Lifetime Average Daily Truck Volume .....	22
Chapter 3	DESCRIPTION, DESIGN, AND HISTORY OF BRIDGE 9340 .....	25
	Description of Bridge .....	25
	Bridge Design .....	27
	History of Bridge .....	28
Chapter 4	FIELD TEST PROCEDURES .....	31
	Location of Strain Gages .....	31
	Test Descriptions .....	35
	Controlled Load Tests .....	35
	Open Traffic Tests .....	39
	Data Collection System .....	40
Chapter 5	SUMMARY OF RESULTS .....	41

	Test 1 Results.....	41
	Test 2 Results.....	41
	Test 3 Results.....	45
	Test 4 Results.....	45
	Open Traffic Results.....	45
	Reversal and High-Tension-Stress Member Results .....	55
Chapter 6	RESULTS OF ANALYSES .....	57
	2-D Analysis of Main Truss.....	57
	Test 2.....	58
	Test 4.....	63
	3-D Analysis of Truss System .....	66
	Possible Problem Members and Remaining Life in Main Truss.....	71
	2-D Analysis of Floor Truss .....	72
	Test 1.....	72
	Test 4.....	74
	Remaining Life of the Floor Truss.....	76
Chapter 7	SUMMARY AND CONCLUSIONS .....	77
Chapter 8	REFERENCES .....	81

## LIST OF FIGURES

Figure 1: Bridge 9340 .....	2
Figure 2: AASHTO Fatigue Resistance Curves .....	9
Figure 3: Possible Cases of $S_{re}$ and $S_{rmax}$ in Relation to the CAFL .....	17
Figure 4: Truck Volume Ratio .....	23
Figure 5: Welded Attachment at Interior of Box Section of Main Truss .....	26
Figure 6: Longitudinal Stiffeners at Floor Truss Connections .....	27
Figure 7: Gaged Locations on the Main Truss.....	32
Figure 8: Gaged Locations on the Floor Truss .....	32
Figure 9: Gaged Upper Chord and Diagonal on Exterior of East Truss.....	33
Figure 10: Data Recording Station on Catwalk of Bridge.....	34
Figure 11: Test Set-ups .....	37-38
Figure 12: Time History of the Response During Test 1 .....	42
Figure 13: Time Histories of the Response During Test 2 .....	43-44
Figure 14: Time Histories of the Response During Test 4 .....	46-48
Figure 15: Largest Stress Event Recorded In Open Traffic Conditions .....	49
Figure 16: Largest Stress Event In High Tension Member .....	56
Figure 17: 2-D Visual Analysis Model of Main Truss .....	57
Figure 18: Distribution of Load Across Bridge Deck.....	59
Figure 19: Comparison of 2-D Analysis and Test Data for Main Truss in Test 2.....	60-61
Figure 20: Comparison of 2-D Analysis and Test Data for Main Truss in Test 4.....	63-64
Figure 21: 3-D SAP2000 Model .....	67

Figure 22: Comparison of 3-D Analysis and Test Data for Main Truss in Test 4.....68-69

Figure 23: 2-D Visual Analysis Model of Floor Truss With Concrete Deck .....73

Figure 24: Comparison of 2-D Analysis and Test Data for Floor Truss in Test 4 .....74-75

# LIST OF TABLES

Table 1: Fraction of Trucks In Outer Lane .....22

Table 2: Observed Average Daily Traffic Growth Rates .....23

Table 3: Stress Range Percentages During Constant Data Collection For the East  
Truss.....51

Table 4: Stress Range Percentages During Constant Data Collection For the West  
Truss.....51

Table 5: Stress Range Percentages During Constant Data Collection For the Floor  
Truss.....51

Table 6: Effective Stress Ranges From Constant Data Collection .....52

Table 7: Stress Range Percentages During Triggered Data Collection For the West  
Truss.....53

Table 8: Stress Range Percentages During Triggered Data Collection For the Floor  
Truss.....53

Table 9: Effective Stress Ranges From Triggered Data Collection.....53

Table 10: Stress Range Percentages During Constant Data Collection For the  
Reversal and High Tension Stress Members .....55

Table 11: Ratio of Actual to Predicted Stress Ranges in the Main Truss For 2-D  
Analysis of Test 2 .....62

Table 12: Ratio of Actual to Predicted Stress Ranges in the Main Truss for 2-D  
Analysis of Test 4 .....65

Table 13: Ratio of Actual to Predicted Stress Ranges in the Main Truss for 3-D  
Analysis of Test 4 .....69

Table 14: Predicted Stress Ranges Exceeding the Fatigue Limit During Test 2 .....71

Table 15: Corrected Predicted Stress Ranges For Problem Members During Test 2.....72

Table 16: Ratio of Actual to Predicted Stress Ranges in the Floor Truss for 2-D  
Analysis of Test 4 .....76

## EXECUTIVE SUMMARY

Bridge 9340 is a deck truss with steel multi-girder approach spans built in 1967 across the Mississippi River just east of downtown Minneapolis. The approach spans have exhibited several fatigue problems; primarily due to unanticipated out-of-plane distortion of the girders. Although fatigue cracking has not occurred in the deck truss, it has many poor fatigue details on the main truss and floor truss systems. Concern about fatigue cracking in the deck truss is heightened by a lack of redundancy in the main truss system. The detailed fatigue assessment in this report shows that fatigue cracking of the deck truss is not likely. Therefore, replacement of this bridge, and the associated very high cost, may be deferred.

Strain gages were installed on both the main trusses and the floor truss to measure the live-load stress ranges. The strain gages were monitored while trucks with known axle weights crossed the bridge and under normal traffic. Two- and three-dimensional finite-element models of the bridge were developed and calibrated based on the measured stress ranges. These finite-element models were used to calculate the stress ranges throughout the deck truss.

The peak stress ranges are less than the fatigue thresholds at all details. Therefore, fatigue cracking is not expected during the remaining useful life of the bridge. The most critical details, i.e. the details with the greatest ratios of peak stress range to the fatigue threshold, were in the floor trusses. Therefore, if fatigue problems were to develop due to a future increase in loading, the cracking would manifest in a floor truss first. Cracks in the floor trusses should be readily detectable since the floor trusses are easy to inspect from the catwalk. In the event that the cracks propagate undetected, the bridge could most likely tolerate the loss of a floor truss without collapse, whereas the failure of one of the two main trusses would be more critical.

This research has implications for bridges other than 9340. The research verified that the behavior of this type of bridge can be deduced with a modest number of strain gages at key locations combined with detailed analyses. This instrumentation plan can be used in other similar bridges. Guidelines for service-load-level analyses of similar bridges are given to estimate typical fatigue stress ranges. Bridges may now be rated for fatigue in accordance with the new Load and Resistance Factor Rating procedures. Fatigue rating should be based on service-load-level analyses conducted according to these guidelines. If the results of preliminary assessment indicate that there is still concern about fatigue, the analyses should be calibrated with limited strain-gage testing.

# CHAPTER 1

## INTRODUCTION

### PROBLEM STATEMENT

Bridge 9340 supports four lanes in each direction (eight lanes total) of I-35W across the Mississippi River just east of downtown Minneapolis. The Average Daily Traffic (ADT) is given as 15,000 in each direction, with ten percent trucks. Bridge 9340 consists of a deck truss and steel multi-girder approach spans built in 1967. The deck truss, shown in Figure 1, has a center span of 139 meters, north and south spans of 80.8 meters and cantilever spans of 11.6 and 10.9 meters. The bridge was designed using the 1961 American Association of State Highway Officials (AASHO) Standard Specifications [1]. At that time, unconservative fatigue design provisions were used. The American Association of State Highway and Transportation Officials (AASHTO) fatigue design rules were substantially improved as a result of research at Lehigh University in the 1970's [2,3].

The approach spans have exhibited several fatigue problems; primarily due to unanticipated out-of-plane distortion of the girders. Although fatigue cracking has not occurred in the deck truss, it has many poor fatigue details on the main truss and floor truss systems.

Stress ranges calculated using the lane load as live load are greater than fatigue thresholds for many of the details. The poor fatigue details in the deck truss include intermittent fillet welds, welded longitudinal stiffeners and welded attachments at diaphragms inside tension members. These details are classified as Category D and E with threshold stress ranges 48 and 31 MPa, respectively.

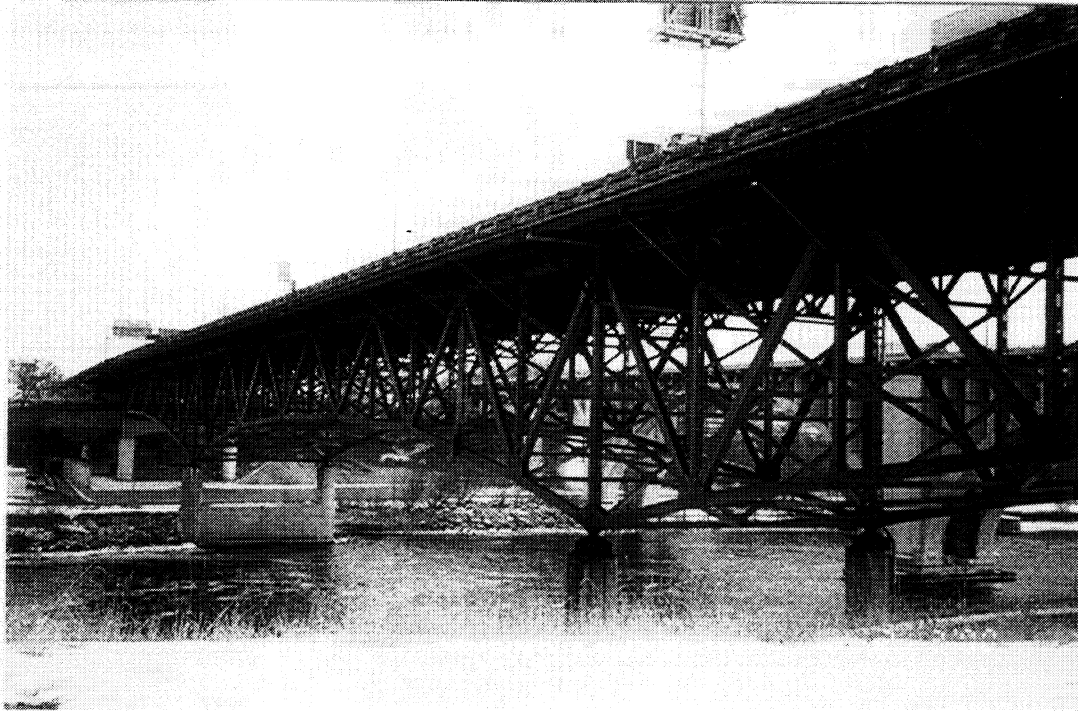


Figure 1: Bridge 9340

The design analysis, using the AASHTO lane load in all lanes, shows design-live-load stress ranges in the truss members much higher than these thresholds. Design-live-load stress ranges were greatest, up to 138 MPa, in members that experience load reversal as trucks pass from the outside spans onto the center span. The predicted average life at that stress range is between 20,000 and 40,000 cycles. With 15,000 trucks per day crossing the bridge in each direction, these details should have cracked soon after opening if the stress ranges were really this high.

The actual stress ranges can be determined by instrumenting the bridge with strain gages and monitoring strains under both a known load and open traffic. Fortunately, the actual stress ranges are much lower than these design live-load stress ranges. Consequently, the fatigue life is far longer than would be predicted based on the design-live-load stress ranges. The difference

between actual and predicted stress ranges is the result of conservative assumptions made in the design process. The primary reason is that the traffic on the bridge is 90 percent cars and weighs a lot less than the lane loading, (9.34 kN/m). The lane loading is approximately equivalent to maximum legal 356 kN trucks spaced at about 38 meters apart.

The lane load may be appropriate for a few occurrences during the life when there are bumper-to-bumper trucks in all lanes, and the bridge should be designed to have sufficient strength to withstand this load. However, a few occurrences of loading of this magnitude would not have a significant effect on fatigue cracking. In fact, it has been shown that essentially infinite fatigue life is achieved in tests when fewer than 0.01 percent of stress ranges exceed the fatigue threshold [4]. Therefore, only loads that occur more frequently than 0.01 percent of the time have an effect on fatigue. If there are 15,000 significant load cycles (trucks) per day, any load that happens less frequently than daily is irrelevant as far as fatigue is concerned. In observing this bridge closely over the period of more than a year, the authors have never seen a condition where there were closely spaced trucks in each lane.

Other reasons that the actual live-load stress ranges are lower than design stress ranges include unanticipated structural behavior at service load levels. This unanticipated behavior includes composite action of the slab and the floor trusses and unintended partial fixity at the piers due to bearings that do not respond to live loads.

Concern about fatigue cracking in the deck truss is heightened by a lack of redundancy in the main truss system. Only two planes of the main trusses support the eight lanes of traffic. The

truss is determinate and the joints are theoretically pinned. Therefore, if one member were severed by a fatigue crack, that plane of the main truss would, theoretically, collapse.

However, it is possible that collapse may not occur if this happened. Loads may be redistributed and joints may resist rotation and develop bending moments. If the fractured main truss deflected significantly the slab could prevent the complete collapse through catenary action. In any event, a fracture in one of the main trusses would require prolonged closure of the bridge and a major disruption.

## **OBJECTIVE OF RESEARCH**

This research was conducted to:

- 1) characterize the actual statistical distribution of the stress ranges;
- 2) evaluate the potential for fatigue cracking in the deck truss and, if there is the potential for cracking, to estimate the remaining life;
- 3) recommend increased inspection or retrofitting, if necessary.

## **SCOPE OF REPORT**

This report covers a literature review, inspection of the deck truss, field-testing and analysis of the deck truss, and discussion of the results. There is a brief discussion of previous problems with the approach spans, otherwise the approach spans are not discussed in detail.

The bridge was instrumented with strain gages, load tested with dump trucks with known axle weights in early October of 1999, and monitored on and off from March to August of 2000 to characterize the statistical distribution of the stress ranges. The measured strains were used to calibrate two and three-dimensional finite-element models of the bridge. These finite-element models were used to calculate the stress ranges throughout the deck truss. These stress ranges were compared to the thresholds for the particular details at each critical location. The most critical details, i.e. the details with the greatest ratios of peak stress range to the fatigue threshold, were identified. Recommendations are made for focused visual inspection.

## CHAPTER 2

### BACKGROUND

#### FATIGUE RESISTANCE

The American Association of State Highway and Transportation Officials (AASHTO) bridge design specifications (both the Standard Specifications and the Load and Resistance Factor Design (LRFD) Specifications) contain similar provisions for the fatigue design of welded details on steel bridges [5,6]. Welded and bolted details are designed based on the nominal stress range rather than the local "concentrated" stress at the weld detail. The nominal stress is usually obtained from standard design equations for bending and axial stress and does not include the effect of stress concentrations of welds and attachments. Since fatigue is typically only a serviceability problem, fatigue design is carried out using service loads. Although cracks can form in structures cycled in compression, they arrest and are not structurally significant. Therefore, only members or connections for which the stress cycle is at least partially in tension need to be assessed.

Both AASHTO bridge specifications are based on the same set of fatigue-resistance curves (S-N curves). The relationship used to represent the S-N curve is an exponential equation of the form:

$$N = A S^{-3} \quad (\text{Eq. 1})$$

or  $\log N = \log A - 3 * \log S$

where:  $N$  = number of cycles to failure,

$A$  = constant dependent on detail category

and  $S$  = applied constant amplitude stress range.

In design, the S-N curves give the allowable stress range for particular details for the specified life or number of cycles. In evaluation of existing bridges, these S-N curves can be used to

estimate of the total number of cycles to fatigue failure for the actual measured stress range at a particular detail. The remaining life can be estimated by subtracting from the total cycles the cycles experienced in the past.

Each S-N curve represents a category of details. The AASHTO specifications present seven S-N curves for seven categories of weld details, Although E', in order of decreasing fatigue strength. Figure 2 shows the S-N curves for the detail categories C, D, E, and E'. (The categories A, B, and B' are usually not severe enough to cause cracking in service and therefore will not be discussed.) The S-N curves are based on a lower bound to a large number of full-scale fatigue test data with a 97.5 percent survival limit. Therefore, a detail optimally designed with these S-N curves and actually exposed to the stress ranges assumed in design has a 2.5 percent probability of cracking during the specified lifetime.

Figure 2 shows the fatigue threshold or constant amplitude fatigue limits (CAFL) for each category as horizontal dashed lines. When constant-amplitude tests are performed at stress ranges below the CAFL, noticeable cracking does not occur. For bridges in service, if almost all the stress ranges are below the CAFL, the fatigue life is considered essentially infinite. The CAFL for Category C, D and E is 69, 48, and 31 MPa, respectively.

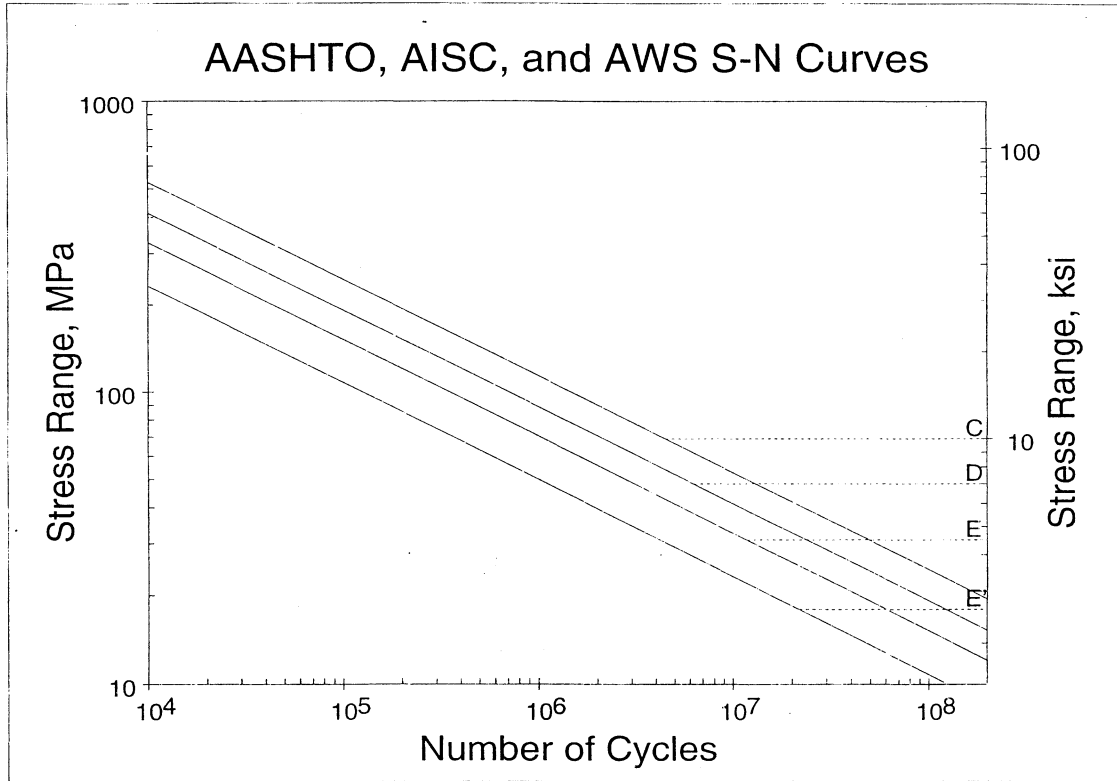


Figure 2: AASHTO Fatigue Resistance Curves

The critical details on Bridge 9340 are classified as non-load-bearing attachment details, i.e. attachments to structural members that do not carry significant load. With the exception of some special cases, these type of attachments are rated Category C if less than 51 mm long in the direction of the primary stress range, D if between 51 and 101 mm long, and E if greater than 101 mm long.

## **STRUCTURAL REDUNDANCY**

In any structural system, loads are carried along a variety of simultaneous paths. The existence of these redundant load paths in a bridge ensures reliable structural behavior in instances of damage to some of the structural elements [7]. However, if there is no redundancy, failure of one member may cause the entire structure to collapse.

The Committee on Redundancy of Flexural Systems conducted a survey of steel highway and railroad bridges reported suffering distress in main load carrying members. Twenty-nine states and six railroad companies responded. A total of 96 structures were reported as suffering some distress. The survey found that most failures were related to connections, nearly all of which were welded. The data collected on bridges that suffered damage indicate that few steel bridges collapse if redundancy is present. The reported collapses involved trusses with essentially no redundancy [7].

In another study, Ressler and Daniels [8] found that the number of fatigue-sensitive details present in the structure significantly affected the system reliability of a nonredundant bridge. For example, the reliability of a span with 20 Category E' details was found to be substantially lower than the reliability associated with a single E' detail.

## **CALCULATED AND ACTUAL BRIDGE RESPONSE**

Many studies have shown that the simplified calculations used to predict stresses in bridge members are inherently conservative [9,10,11,12,13,14,15,16]. As a result, the calculated stresses are often much higher than the actual service stresses and the fatigue assessment is unnecessarily pessimistic. From the form of Equation 1, it is clear that a small change in the estimate of the stress range results in a much larger change in the life, i.e. the effect is cubed. For example, if the stress range is conservative by only 20 percent, the computed life will be 42 percent too low.

The design calculations, load models, and the level of conservatism are appropriate for strength design where there is great uncertainty in the maximum lifetime loads. However, for fatigue evaluation of an existing bridge, an accurate estimate of the typical everyday stress ranges is required. Therefore, for fatigue evaluation of existing bridges, a more appropriate set of analysis assumptions is required and it is best if the analysis is “calibrated” relative to measured strain data.

In a large bridge, service live-load stress ranges typically do not exceed 20 MPa [10]. The stress ranges are small because the dimensions of the members of a large bridge are typically governed by dead loads and strength design considerations. Since the strength design must account for a single worst-case loading scenario over the life of the bridge, conservative load models are used (large factors of safety).

In addition to conservative load models, assumptions in analysis can also often lead to actual stresses being far lower than predicted stresses. An example of the effect of these assumptions is illustrated in a study of U.S. Highway 69 in Oklahoma crossing the South Canadian River [11]. Concerns of fatigue damage arose when poor welding techniques had been used in the widening of the bridge. Preliminary analyses had shown that stress ranges could exceed allowable stress ranges at over 100 locations on the bridge. However, when the bridge was instrumented with strain gages and monitored under known loads and normal traffic the largest measured stress range was found to be 27 percent of the allowable stress range, far below predicted.

In another study, fatigue concerns arose due to a considerable amount of corrosion on the floorbeams of Bridge 4654 in Minnesota [12]. The bridge was instrumented with strain gages and monitored under known loads and normal traffic. Here, measured stress ranges ranged from 65 to 85 percent of those predicted by analysis.

These disparities are due to the fact that analytical models often use assumptions that conservatively neglect ways in which the structure resists load. Sometimes the structural behavior could never have been predicted in design. For example, Dexter and Fisher [13] discuss the results of field tests on an adjacent pair of railroad bridges. It was found that ballast had fallen in the narrow space between the girders forcing the adjacent bridges to deflect together as if joined. This behavior distributed load from the bridge with the train on it to the other bridge, resulting in stress ranges less than half of predicted, especially in the exterior girder nearest the adjacent bridge.

In a study performed by Brudette et al. [14], more than 50 years of bridge test data were collected and examined to determine specific load-resisting mechanisms that are typically ignored in design or evaluation. The study revealed that lower stress ranges in a structure can be attributed to unintended composite action, contributions from non-structural elements such as parapets, unintended partial end fixity at abutments, and direct transfer of load through the slab to the supports.

- **Composite Action:** Bridges with shear connectors at the slab-girder interface typically display full composite action. However, some composite action is seen in the absence of shear connectors, resulting in lower stresses in the structure. At service load levels, composite action is even effective in resisting negative moment.
- **Partial End Fixity:** Often, bridges and bridge members are designed to behave as if they are simply supported. However, these supports usually do not behave as intended. Partial fixity in the end connections on beams causes a lower positive moment that would be obtained from the simply supported beam model. Bearings that are meant to be a roller boundary condition, or fixing the displacement in the vertical direction while allowing longitudinal movement, can become frozen due to corrosion, extremely cold weather or poor design. This can change the response of a bridge subjected to loading by introducing horizontal resistance where it was not intended.
- **Transfer of Load Through Slab:** Load distribution refers to the lateral distribution of load to longitudinal supporting elements. The slab typically does a much better job of

spreading the load than anticipated in design. The lateral distribution is more favorable than assumed, and there is significant spreading of the load longitudinally, which is not even counted on in design. Often, part of the load is distributed directly to the supports bypassing the longitudinal stringers or girders.

In a similar study, the Ministry of Transportation of Ontario conducted a program of bridge testing that included more than 225 bridges over a period of many years [15]. The study revealed that in every bridge test there were surprising results that were not expected the most common of which was a bridge's ability to sustain much larger loads than their estimated capacities.

Specifically, the following observations were made in the testing of steel truss bridges.

- The stringers of the floor system sustained a large share of the tensile force thus reducing the strains felt by the chord in contact with the floor system.
- Again, composite action in non-composite systems was shown to exist. However, subsequent tests showed that this composite action breaks down completely as the failure limit state for the girder is approached [16].

Although these unintended structural behaviors are nearly impossible to model, they often combine to produce actual stresses well below those calculated by simplified design calculations or even finite-element analysis of the idealized structure [10].

To calibrate the analysis, the results are compared to the measured response and changes are made in the model until the results agree reasonably well with the measurements. Strain gage data are typically acquired on several bridge members where maximum stress ranges are expected to occur. Measurements are typically made while a truck or multiple trucks of known weight and configuration traverse the bridge in the absence of other traffic. The results from this test eliminate uncertainty in the load and isolate the part of the error due to the analysis. The analysis is linear, so once it is calibrated it can be used to predict the stress ranges from the maximum legal load, permit loads, or groups of trucks as appropriate for the fatigue analysis.

Often, some measurements are also made in open traffic for several days to characterize the statistical distribution of the topical stress ranges, which is proportional to the statistical distribution of the truck axle weights or total gross weights. Some members (e.g. floorbeams) are loaded by each truck axle. The members of a large trusses such as bridge 9340 do not respond to each axle load separately but rather respond with one cycle associated with the gross vehicle weight.) In highway bridges, a two or three day period seems to be satisfactory to capture a realistic representation of stress ranges and their respective frequencies [17]. It is best if the data collection system is left running continuously to capture both day and night traffic with both full and empty trucks. It may also be wise to capture seasonal changes in traffic and the response of the bridge by taking data in two or three day periods at various times of the year.

Once strain data at known locations has been accumulated, a finite element model of the bridge is generated. The model must be created with as much accuracy as possible before calibration

begins. The model is then calibrated by adjusting: 1) the amount of composite action in members near the deck; 2) the fixity of the supports; and, 3) the distribution of loads on the deck; until calculated strains match measured strains. Once the model is calibrated by a limited number of measurements, it can be used to calculate strains throughout the bridge.

## **FATIGUE EVALUATION PROCEDURES**

An actual service load history is likely to consist of cycles with a variety of different load ranges, i.e., variable-amplitude loading [4]. However, the S-N curves shown in Figure 2 are based on constant-amplitude loading. There is an accepted procedure for converting variable stress ranges to an equivalent constant-amplitude stress range with the same number of cycles. This procedure is based on the damage summation rule jointly credited to Palmgren and Miner (referred to as Miner's rule) [18]. If the slope of the S-N curve is equal to three, then the relative damage of stress ranges is proportional to the cube of stress range. Therefore, the effective stress range is equal to the cube root of the mean cube of the stress ranges [19].

$$S_{re} = (\sum p_i S_{ri}^3)^{1/3} \quad (\text{Eq. 2})$$

The effective stress range is used the same way as the constant amplitude stress range, i.e. the S-N curve is entered with the value of the effective stress range and the intersection with the S-N curve defines the number of cycles in the total life, assuming that the effective stress range is relatively constant over the life. This procedure works fairly well in the shorter life regime where the effective stress range is much larger than the fatigue threshold.

When the effective stress range is on the order of the fatigue threshold or less, dealing with variable stress ranges becomes more complicated. Figure 3 shows the lower part of an S-N curve with three possible variable stress-range distributions superposed [20]. The effective stress range is shown as  $S_{re}$  in this figure and is used the same way as a constant-amplitude stress range with the S-N curves in the finite-life regime (Case 1 and Case 2).

For Case 3 in Figure 3, essentially all the stress ranges are less than the CAFL. In this case, long-life variable-amplitude fatigue tests on full-scale girders with welded details show that if less than one in 10,000 cycles exceed the CAFL, then essentially infinite life is obtained [4]. This phenomenon is the basis of what is called the “infinite-life” approach, which is incorporated in the AASHTO LRFD specifications [5].

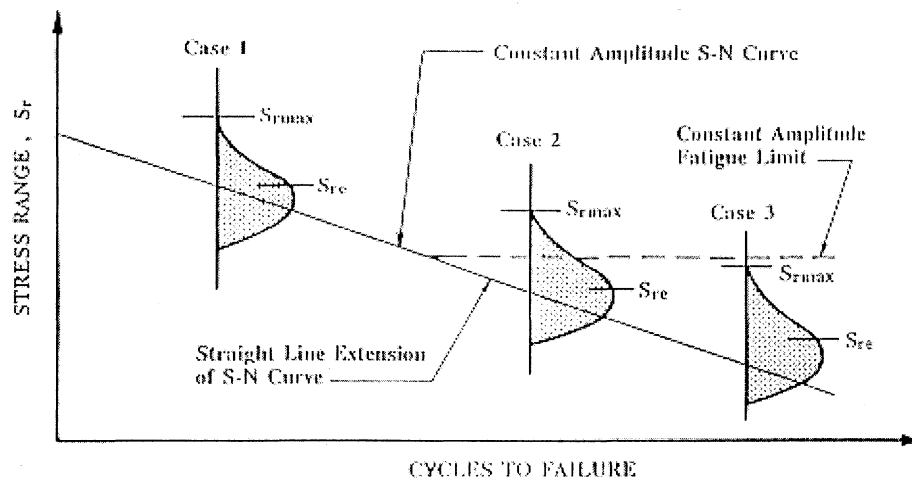


Figure 3: Possible Cases of  $S_{re}$  and  $S_{rmax}$  in Relation to the CAFL

## **Guide Specifications for the Fatigue Evaluation of Existing Bridges**

Fatigue evaluation procedures for existing steel bridges were developed in a project sponsored by the National Cooperative Highway Research Program (NCHRP) that resulted in Report 299 [10]. This study was done to develop practical procedures that accurately reflect the actual fatigue conditions in steel bridges, which could be applied for evaluation of existing bridges or design of new bridges. The procedures utilized information gained from several years of research on variable-amplitude fatigue behavior, high-cycle, long-life fatigue behavior, actual traffic loadings, load distribution, and assessment of material properties and structural conditions.

In NCHRP 299, it is stated that fatigue checks should be based on typical conditions that occur in the structure, rather than the worst conditions expected to occur as in a strength design. The procedure begins with determination of a nominal stress range for the truck traffic crossing the bridge. This stress range is then compared to the S-N curve for the type of detail found on the structure to determine the number of cycles to failure. Then the life of the detail can be calculated using current estimated truck volume, the present age of the bridge, and the number of load cycles for each truck passage.

NCHRP report 299 provides the following equation to calculate fatigue life for an estimated lifetime average daily truck volume based on stress range measurements taken at the bridge site.

$$Y_f = [(f K \times 10^6) / (T_a C (R_s S_{re})^b)] - a \quad (\text{Eq. 3})$$

where,

$Y_f$  = remaining fatigue life in years

$S_{re}$  = effective stress range

$R_s$  = reliability factor

$C$  = stress cycles per truck passage

$K$ ,  $b$ , and  $f$  = fatigue curve constants

$T_a$  = estimated lifetime average daily truck volume

$a$  = present age of bridge in years

Further discussion of these variables follows.

### **Effective Stress Range**

The effective stress range is calculated from Equation 2 using stress-range histograms obtained from field measurements on the bridge under normal traffic. The stress range may be computed from an analysis where the loading is the cube root of the mean cube of the gross-vehicle-weight histogram. Alternatively, an HS-15 truck (HS-20 loading multiplied by 0.75) may be used to calculate the effective stress range if measurements are not available.

## Reliability Factor ( $R_s$ )

The reliability is used when calculating the remaining safe life. It is used to ensure that the actual life will exceed the safe life to a desired probability. When calculating the remaining mean life, the reliability factor is 1.0: When calculating the remaining safe life, multiply the computed stress range  $S_{re}$  by a reliability factor:

$$R_s = R_{s0} (F_{s1}) (F_{s2}) (F_{s3}) \quad (\text{Eq. 4})$$

where,

$R_s$  = reliability factor associated with calculation of stress range

$R_{s0}$  = basic reliability factor

= 1.35 for redundant members

= 1.75 for nonredundant members

$F_{s1}$  = 0.85 if effective stress range calculated from stress range histograms obtained from field measurements

= 1.0 if effective stress range calculated by other methods

$F_{s2}$  = 0.95 if loads used in computations are for site-specific weigh-in-motion measurements

= 1.0 if the AASHTO fatigue truck is used

$F_{s3}$  = 0.96 if rigorous analytical method is used to determine load distribution

= 1.0 if approximate method based on parametric studies is used

### **Stress Cycles Per Truck Passage (C)**

A single truck traveling over a bridge can often have a complex response resulting in more than one stress cycle per truck passage. Whereas most main members feel just one cycle per truck, transverse members near the deck may feel each axle load as it passes. The number of stress cycles per truck passage, C, has been determined for various types of bridge members. The number of stress cycles per passage for Bridge 9340, a deck truss bridge, is 1.0.

### **Fatigue Curve Constants (K, b and f)**

The equation for the S-N curves was given in Equation 1. The parameter b is the exponent and is 3.0 for the AASHTO S-N curves. For convenience in calculating the remaining life in years, the detail constant K is used (Eq. 5).

$$K = A / [365 \times 10^6] \quad (\text{Eq. 5})$$

Where A was defined for Equation 1. There is considerable scatter in the fatigue data on which Eq. 4 is based. It is normally assumed that the scatter in stress range values follows a log-normal statistical distribution for a given N. Consequently, allowable nominal stress ranges are usually defined two-standard deviations below the mean stress ranges. Since the mean and allowable S-N curves for a given detail are assumed to be parallel on a log-log plot, the ratio of stress ranges for the two curves is the same at all cyclic lives [10].

The constant f is used to modify the constant K to reflect the mean remaining life rather than the safe remaining life. The constant f equals the ratio of the mean-life curve intercept, A', to the safe-life curve intercept, A. For categories B through E', the ratio of mean to allowable stress

range does not vary greatly and averages 1.243. Because of the power of 3 in the S-N curve, the corresponding ratio of mean to safe lives is equal to 1.243 cubed, or 1.92. Thus, the value of  $f$  is taken as 2.0 while calculating mean life. If the safe life is being calculated,  $f$  equals 1.0 [10].

### **Lifetime Average Daily Truck Volume ( $T_a$ )**

The present average daily truck volume in the outer lane,  $T$ , can be calculated from the ADT at the site as follows:

$$T = (ADT) F_T F_L \quad (\text{Eq. 6})$$

where

ADT = present average daily traffic volume in both directions

$F_T$  = fraction of trucks in the traffic

$F_L$  = fraction of trucks in the outer lane

The ADT can be determined by doing a traffic count or may be obtained from Department of Transportation data for the location of interest. The fraction of trucks in the traffic is suggested to be 0.20 for rural interstate highways, 0.15 for rural highways and urban interstate highways, and 0.10 for urban highways. The fraction of trucks in the outer lane may be determined from Table 1.

Table 1: Fraction of Trucks in Outer Lane [10]

Number of Lanes	2-Way Traffic	1-Way Traffic
1	-	1.00
2	0.60	0.85
3	0.50	0.80
4	0.45	0.80
5	0.45	0.80
6 or more	0.40	0.80

Using the calculated present average daily truck volume in the outer lane,  $T$ , the annual growth rate,  $g$ , the present age of the bridge,  $a$ , and Figure 4, the lifetime average daily truck volume in the outer lane can be determined. The annual growth rate can be determined from Table 2. This table lists annual growth rates estimated from Annual Average Daily Traffic (AADT) data taken at counting stations throughout the United States between the years 1938 and 1985.

Table 2: Observed Average Daily Traffic Growth Rates [10]

Type of Highway	Rural or Urban	Growth Rate %
Interstate	Rural	4.45
	Urban	4.98
U.S Route	Rural	2.87
	Urban	4.19
State Route	Rural	3.77
	Urban	3.27

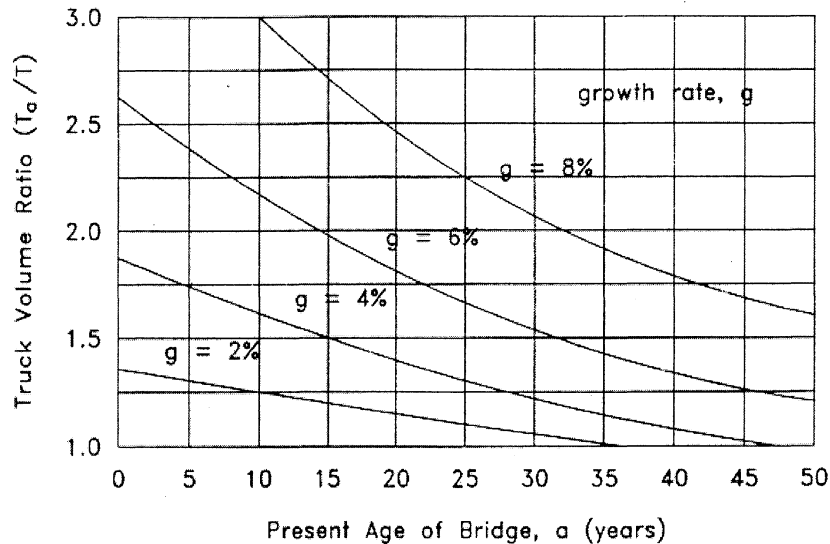


Figure 4: Truck Volume Ratio ( $T_a / T$ ) [10]

## CHAPTER 3

### DESCRIPTION, DESIGN, AND HISTORY OF BRIDGE 9340

#### DESCRIPTION OF BRIDGE

Bridge 9340 carries I-35W over the Mississippi River just east of downtown Minneapolis. Constructed in 1967, the 581 meter long bridge has 14 spans. The south approach spans (Spans #1-#5) are steel multi-beam. The main spans (Spans #6-8) consist of a steel deck truss. The north approach spans include both steel multi-beam (Spans #9-#11) and concrete slab span (Spans #12-14).

There are two steel deck trusses. Most of the truss members are comprised of built-up plates (riveted) while some of the diagonal and vertical members are rolled I-beams. The connections include both rivets and bolts. The truss members have numerous poor welding details. Recent inspection reports have noted corrosion at the floorbeam and sway brace connections, and pack rust forming between connection plates [21].

The bridge deck above the deck truss is 32.9 meters wide from gutter to gutter. Three continuous spans cross the river, the north and south span measuring 80.8 meters and central span measuring 139 meters. Three of the four piers supporting the river crossing have two huge geared rollernest bearing assemblies while the second pier from the north is a fixed connection. These truss bearings have moderate corrosion [21].

The two main trusses have an 11.6-meter cantilever at the north and south ends. There are also 27 floor trusses, spaced at 11.6 meters. These floor trusses frame into the vertical members of

the main truss. The floor trusses consist of WF-shape members and have a 4.97-meter cantilever at each end.

The built-up box sections have attachments measuring 8.9 cm square welded to diaphragms at the interior of all tension members (Figure 5). There are also intermittent fillet welds at the interior of all box sections. These are both Category D details. The floor truss members have longitudinal stiffeners measuring 30.5 cm, which would be considered a Category E detail (Figure 6).

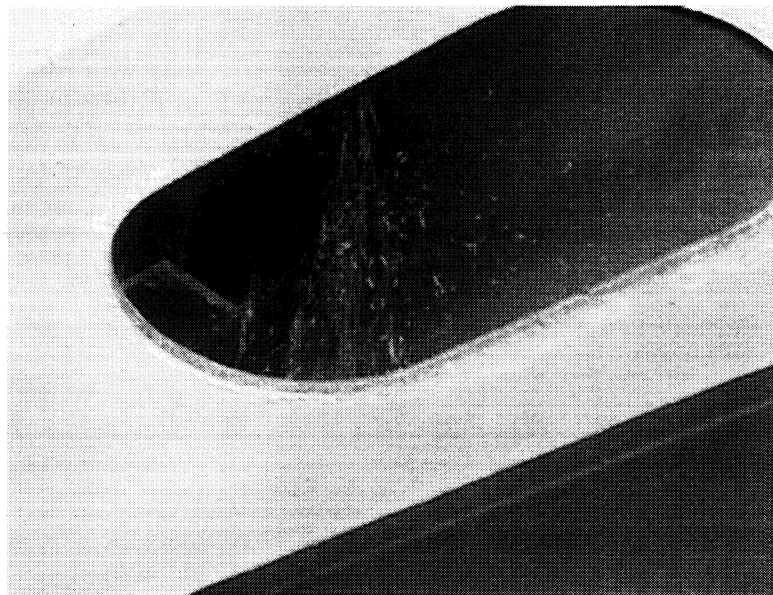


Figure 5: Welded Attachment at Interior of Box Section of Main Truss

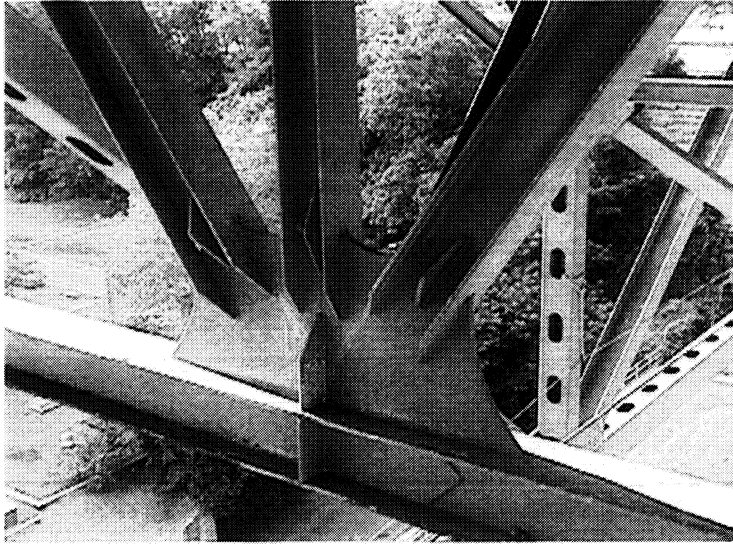


Figure 6: Longitudinal Stiffeners at Floor Truss Connections

## **BRIDGE DESIGN**

Bridge 9340 was designed using the 1961 AASHO specifications [1]. This code utilizes a uniform lane load and a truck for live load. The uniform live load consists of a 9.34 kN per linear meter of load lane and a concentrated load of 11.6 kN for shear. The truck load uses HS-20 truck which has a front axle load of 35.6 kN followed 4.27 meters behind by a 142.3 kN axle followed anywhere from 4.27 to 9.14 meters behind by another 142.3 kN axle. The wheels of the HS-20 truck are spaced 1.83 meters apart. All loads are patterned for maximum effect. Resulting load effects are reduced by ten percent if the maximum load effect is produced by loading three lanes, and by 25 percent if four or more lanes are loaded.

The design of the main trusses utilized the uniform lane loads. All four lanes above the truss being designed and the three nearest lanes opposite the centerline were loaded. Using a tributary length of 11.6 meters for each panel point of the truss, this loading results in a concentrated load of 367 kN and a uniform load of 343.8 kN. The south cantilever of the main truss has a tributary length of 16.6 meters and thus a uniform design load of 489.3 kN. The north cantilever of the main truss is designed using four loaded lanes and a tributary length of 25.5 meters and does not consider the effect of the floor truss cantilever as most of the tributary length is outside of the truss region. This results in a uniform design load for the north cantilever of 716.2 kN.

Load is distributed from the floor system to the floor truss through the stringers. The stringers are continuous over four spans from panel points 0 to 8 and 8' to 0' and continuous over six spans from panel points 8 to 8'. The internal reactions of the four span continuous stringers were found under a HS-20 truck loading and applied to the floor truss in design. Each axle is spaced at 4.27 meters in the design. The HS-20 trucks were then placed in the lanes either shifted toward the curb or the centerline of the roadway to get the maximum load possible on each stringer and to each node in the floor truss. An impact factor of 30 percent was included in the design.

## **HISTORY OF BRIDGE**

Bridge 9340 was built in 1967. While there have been no structural problems with the deck truss, there have been recent problems with the approach spans on both ends of the bridge. In 1997, cracks were discovered in the cross girder at the end of the approach spans. A small section of the end of each main truss is attached to bearings at reinforced openings in the cross

girder. It appeared that resistance to movement of the bearings was causing significant out-of-plane forces and associated distortion on the cross girder, leading to cracks forming at the termination of the stiffeners reinforcing the opening. The cross-girder was retrofit by drilling holes at the tips of the cracks and adding struts from the reinforcing stiffeners back to the girders to reduce the distortion. This retrofit has been successful so far in preventing further crack propagation.

One year later, web gap cracking was discovered at the top of diaphragm attachment plates where they were not welded to the top flange in negative moment areas of the continuous girders. One crack had grown nearly the full depth of one of the girders. This girder was retrofit by drilling a large hole at the crack tips and bolting large web doubler plates to reinforce the cracked area. Other smaller cracks discovered at that time had holes drilled at their ends. Additional holes were drilled in the connection plates and the diaphragms in the negative moment areas were placed much lower to increase the flexibility. The bolts were replaced with the next size lower and were only tightened to a snug condition to allow some slip. Strain gages were placed in the web gap regions of the girder webs to read the values of strain before and after the retrofit. Before the retrofit, stress ranges were large enough to explain the cracking. These stress ranges were reduced by more than 50 percent by the retrofit to levels that would not be expected to cause further cracking [22].

The presence of birds has caused some concern for the deck truss. The main truss is constructed of built-up box sections that in the past have housed many pigeons. It is known that guano can have highly corrosive effects on steel and that extreme corrosion can lead to fatigue problems. Therefore, in the summer of 1999 when the bridge was painted, the access holes of the box sections were fitted with covers to prevent birds from entering the truss members.

## CHAPTER 4

### FIELD TEST PROCEDURES

#### LOCATION OF STRAIN GAGES

Due to the ease of access provided by the transverse catwalk, panel point 10 was chosen for the placement of strain gages. This is located in the negative moment region of the continuous three span truss, therefore the lower chord would be expected to be in compression and the upper chord would be in tension under loading.

Six gages were put on each of the east and west main trusses and the floor truss. On the main trusses, a gage was placed on the interior and exterior of the members at mid-depth, to avoid any bending effects. An upper chord (U8-U10), a diagonal (L9-U10), and a lower chord (L9-L11) were instrumented. These members are identified in Figure 7 as the bold members next to panel point 10. The gages were placed at least one section depth away from the connection to avoid stress concentrations.

The floor truss has gages on the east side of the centerline. A gage was placed on the upper and lower flanges of an upper chord (U5-U6), a diagonal (U5-L7), and a lower chord (L4-L7) (Figure 8). These gages were also placed at least one section depth away from the connection to avoid stress concentrations. Figure 9 shows the gages in place on the exterior of the east truss on the upper chord and the diagonal.

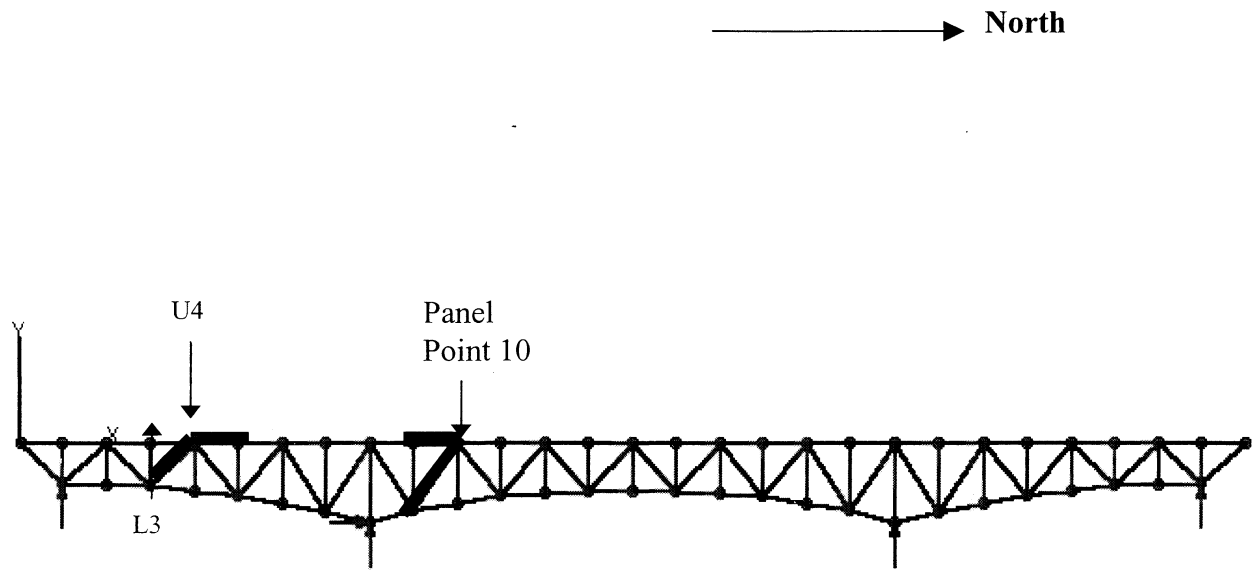


Figure 7: Gaged Locations on the Main Truss

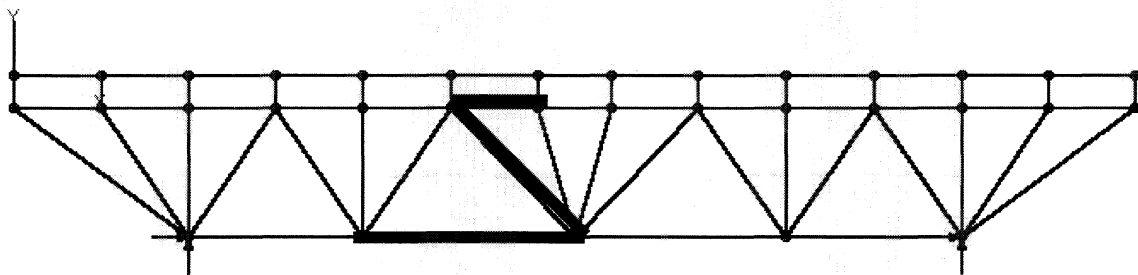


Figure 8: Gaged Locations on the Floor Truss

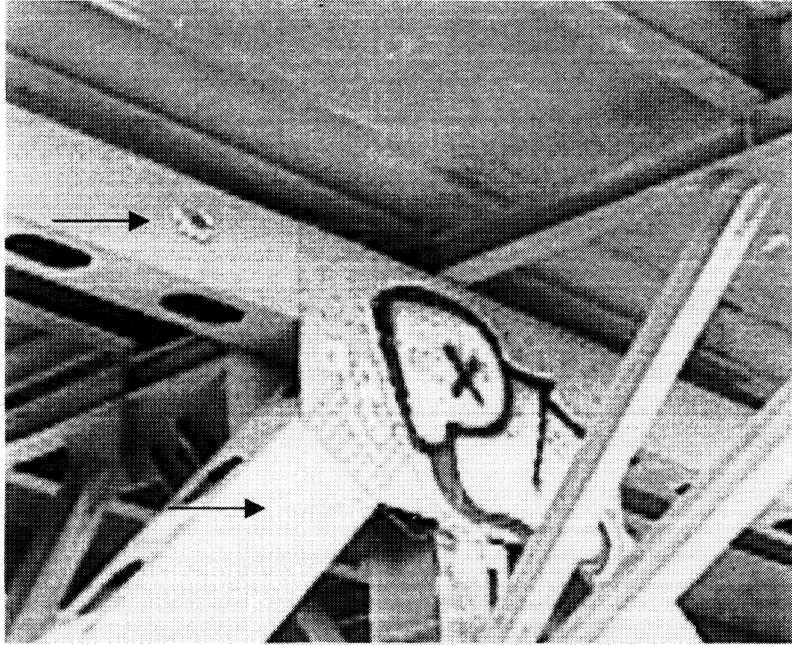


Figure 9: Gaged Upper Chord and Diagonal on Exterior of East Truss

A reversal member (U4-U6) was instrumented, i.e. a member that experiences stress in one direction from approaching trucks and stress in the other direction when the trucks pass over the pier. A member with very high design stress ranges in tension (L3-U4) was also instrumented. These members were located on the south side of the west truss and are designated in bold in Figure 7. Gages were attached to the interior and exterior of these members at mid-depth, also at least one section depth away from the connection.

The wires leading from the gages ran to a central point on the transverse catwalk where they were wired into a data acquisition system housed in a locked electrical box. The box was attached to the catwalk railing using U-bolts. This set up is shown in Figure 10.



Figure 10: Data Recording Station on Catwalk of Bridge

## **TEST DESCRIPTIONS**

### **Controlled Load Tests**

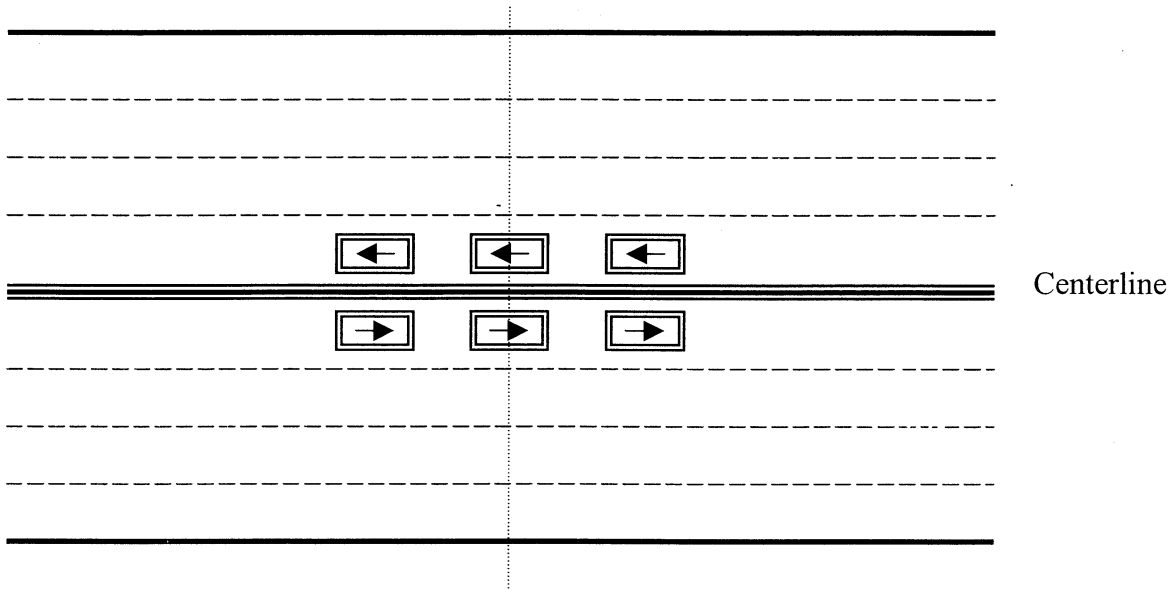
Over the course of two days, four types of tests were conducted. All tests took place after midnight to minimize interference with traffic. Nine Minnesota Department of Transportation (Mn/DOT) tandem-axle dump trucks, each with a gross vehicle weight 227 kN, were used. Strains for this test were recorded for the gages at panel point 10 only, not at the reversal and high-tension-stress members.

Test 1 consisted of two groups of three trucks, with each set driving in a single file line in the left lane in each direction of traffic. This test required that the left lanes were closed. This was done with signing and traffic control provided by Mn/DOT. To represent static conditions each line of trucks were traveling at a crawling speed. The trucks were to follow each other as closely as possible. Optimally, the middle trucks in each group were to meet simultaneously at panel point 10, directly above the instrumented floor truss (Figure 11a).

Test 2 consisted of running all nine trucks in a 3 x 3 formation. The trucks were to travel as close as possible to each other while maintaining highway speeds. Three round trips were made, i.e. three trips in the southbound direction and three in the northbound direction. No lane closures were required for this test. This test set up is shown in Figure 11b.

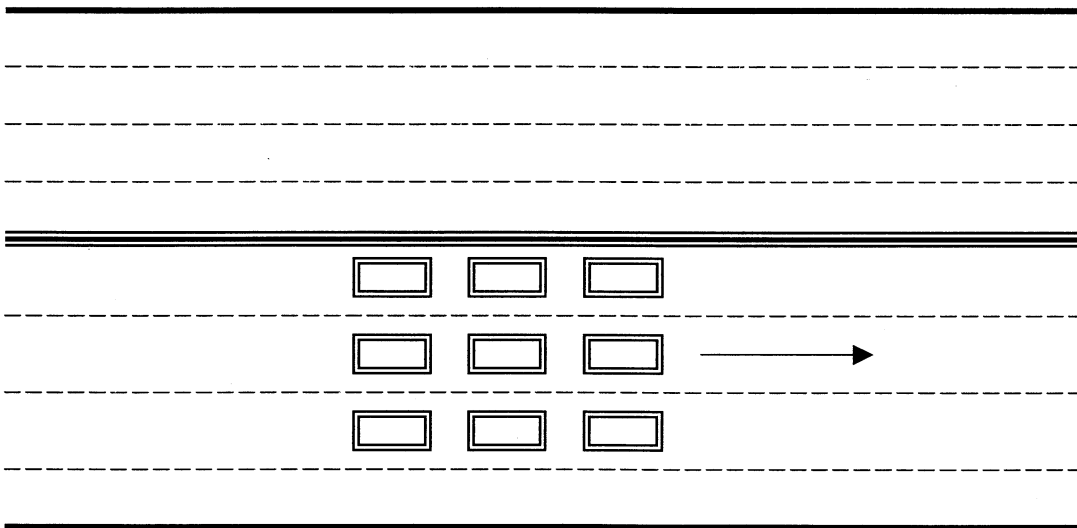
Test 3 consisted of using all nine trucks and running them in a single file line as close as possible to each other (Figure 11c). This was done in the third lane from the centerline as it was the lane most directly over the main truss. The test was run at highway speeds with no lane closures.

In Test 4, the trucks ran side-by-side in groups of three. All nine trucks were used with each group of three following the preceding group by no less than one-half mile. This was done to ensure that only one group of three would be on the bridge at a time. This test was also run at highway speeds. No lane closures were required for this test. The set-up is shown in Figure 11d.

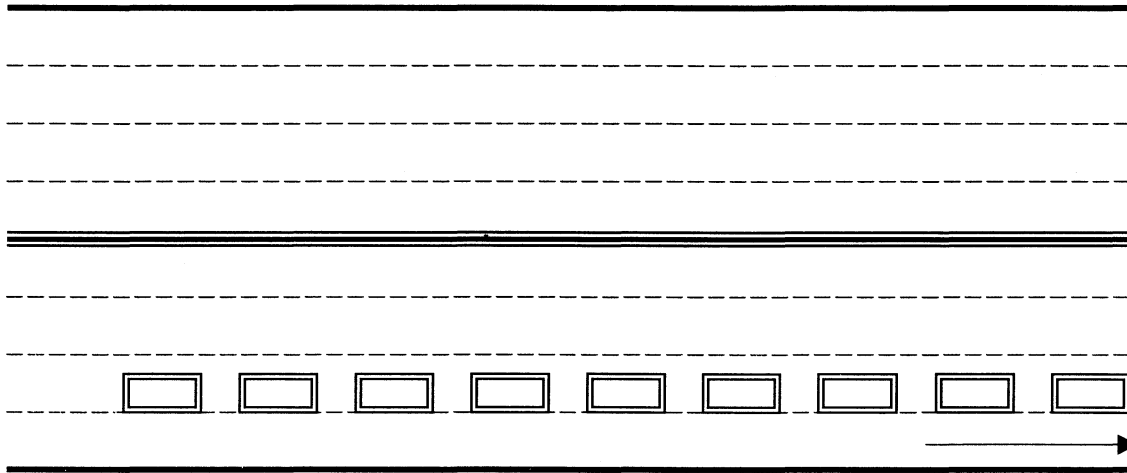


Panel Point 10

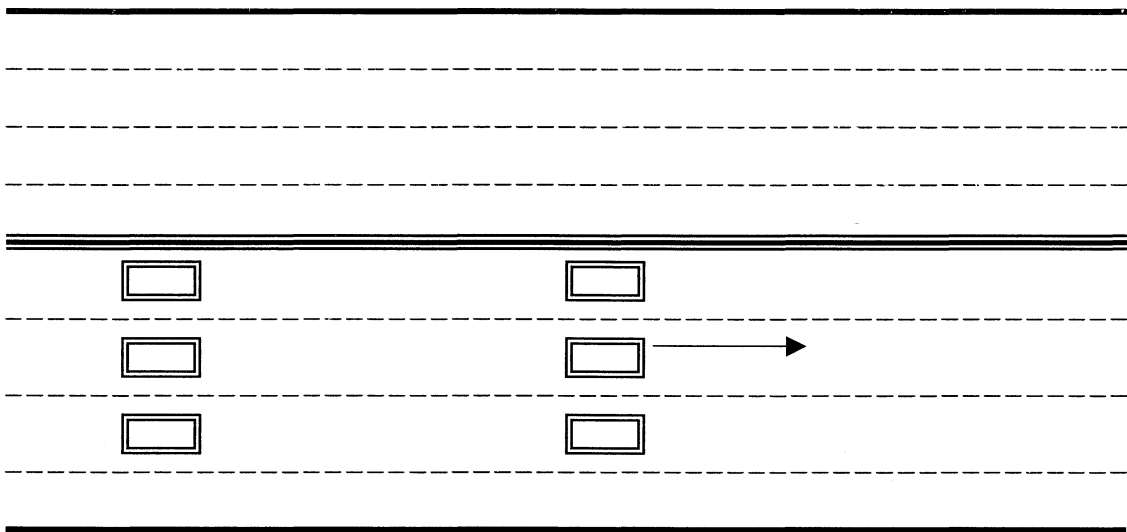
A



B



C



D

Figure 11: Test Set-ups

## **Open Traffic Tests**

Data were also collected during a period of several months on the main and floor trusses to determine typical bridge stress ranges. Both triggered and constant data collection was used. However, triggered data collection was used most to avoid collecting hundreds of megabytes of data that did not show any stress events. This was done for all the gages at panel point 10.

Triggered data collection refers to a method in which the data acquisition system is constantly scanning the gages but does not record anything until strain in a chosen gage exceeds a predetermined limit. The data collection software limited the number of gages one could use as a trigger to three, therefore, one gage on each of the trusses was used as a trigger. In both of the main trusses and in the floor truss, the lower chord was chosen for triggering. This is due to the fact that these chords typically display the highest stress ranges.

The gages on the reversal and the high-tension members were monitored using constant data collection on two separate occasions for about two hours each time. Since these members were such a great distance from the electrical enclosure, taking sample data separately from the gages at panel point 10 proved to be more practical. Therefore a temporary data collection station was set up in a vehicle parked on the walkway below these members. Lead wires were simply dropped to this vehicle during data collection.

## **Data Collection System**

For the truck tests conducted, data were collected using a Campbell Scientific CR9000 data logger. This system is a high-speed multi-channel digital data acquisition system with 16-bit resolution. During these tests, data were collected on between 4 and 18 strain gages at sampling rates of 50 Hz. Running the CR9000 off of its battery gave a cleaner signal than with electrical power. All data were temporarily stored on PCMCIA cards installed on the logger. The data were subsequently copied to a laptop at the end of each test for processing and back-up.

Data were also collected during the long-term monitoring of the bridge using the CR9000 logger. Since the logger was left running for more than a week before the PCMCIA cards were retrieved for data conversion, running off the logger's battery was impossible. Therefore, a temporary power supply running off the bridge's navigational lights was installed and supplied by Mn/DOT. Using external power produced noise in the signal, therefore, to reduce the noise levels in the data a surge protector with a line filter was used.

## CHAPTER 5

### SUMMARY OF RESULTS

#### TEST 1 RESULTS

The goal of the first test was to get the greatest response possible under static conditions in the floor truss. Figure 12 shows a time history of the lower chord in the floor truss during this test. There was a discontinuity in the recording before and after the trucks were in position, making it appear as though the load is applied instantly instead of slowly increasing as the trucks neared the gages. The measured strains show that the lower chord goes into tension as expected. The peak stress range is 28 MPa, which is actually the largest stress range recorded in any member in any test.

#### TEST 2 RESULTS

The goal of the second test was to get the greatest response possible in the main truss. The trucks were driven in the three by three pattern to get a very dense distributed load in all lanes. The measured strains show that the lower chord goes into compression as expected. The greatest stress ranges from this formation of trucks took place in the lower chord and measured 13 MPa. The time history of the response in the lower chord is shown in Figure 13a.

Figures 13b and 13c show the stress ranges in the diagonal and upper chord from the truss during the same event. The stress ranges in the diagonal and upper chord during this test were 10 and 8 MPa, respectively.

### Test 1; Lower Chord of Floor Truss

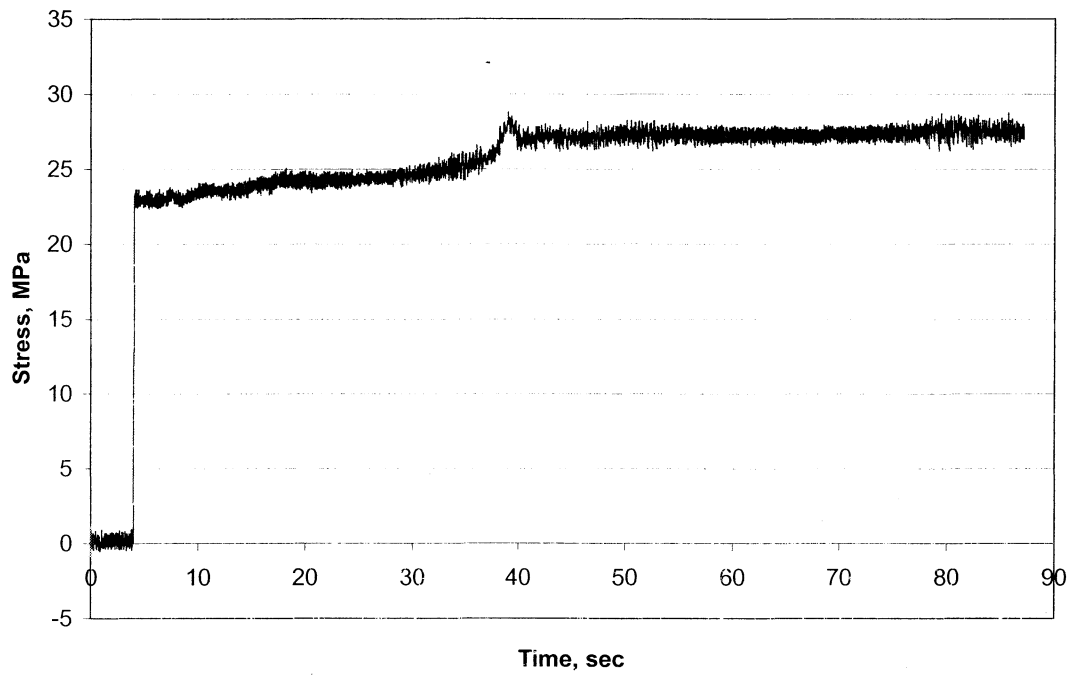
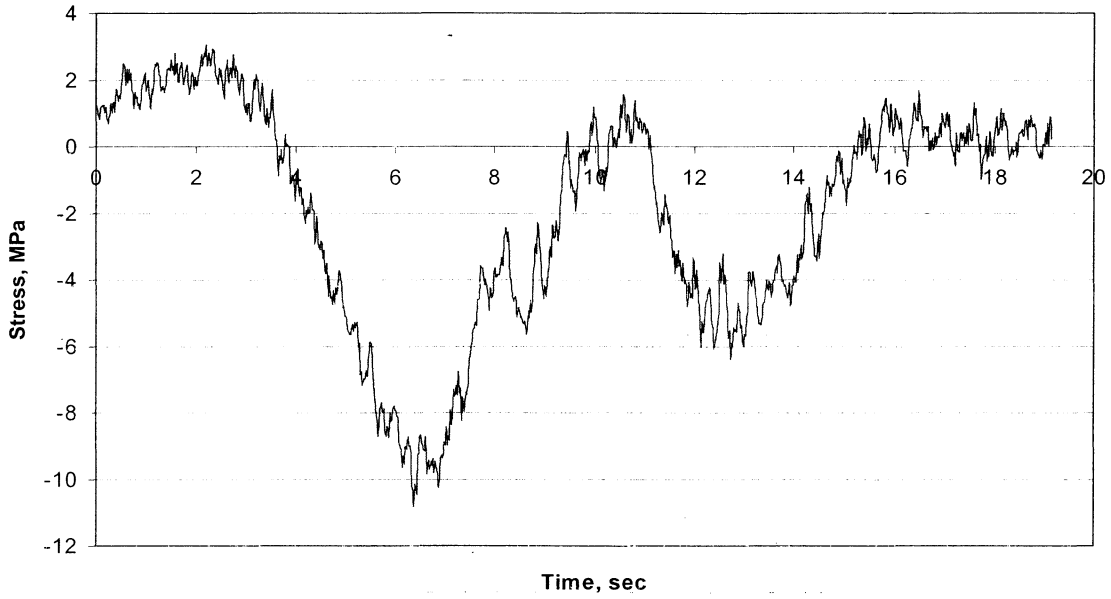


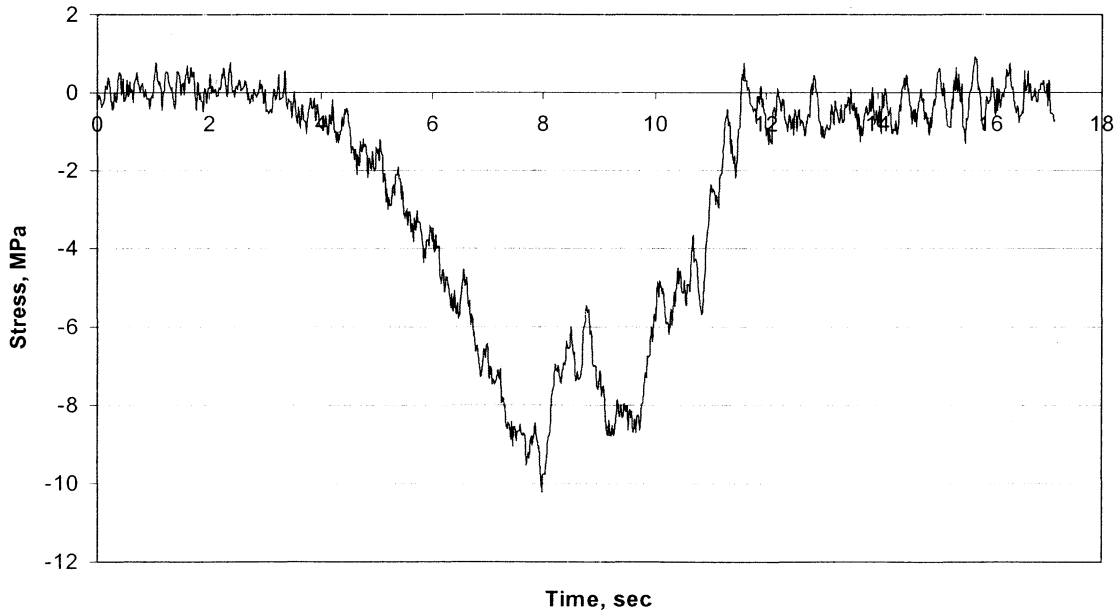
Figure 12: Time History of the Response During Test 1

**Test 2; Lower Chord of West Truss**



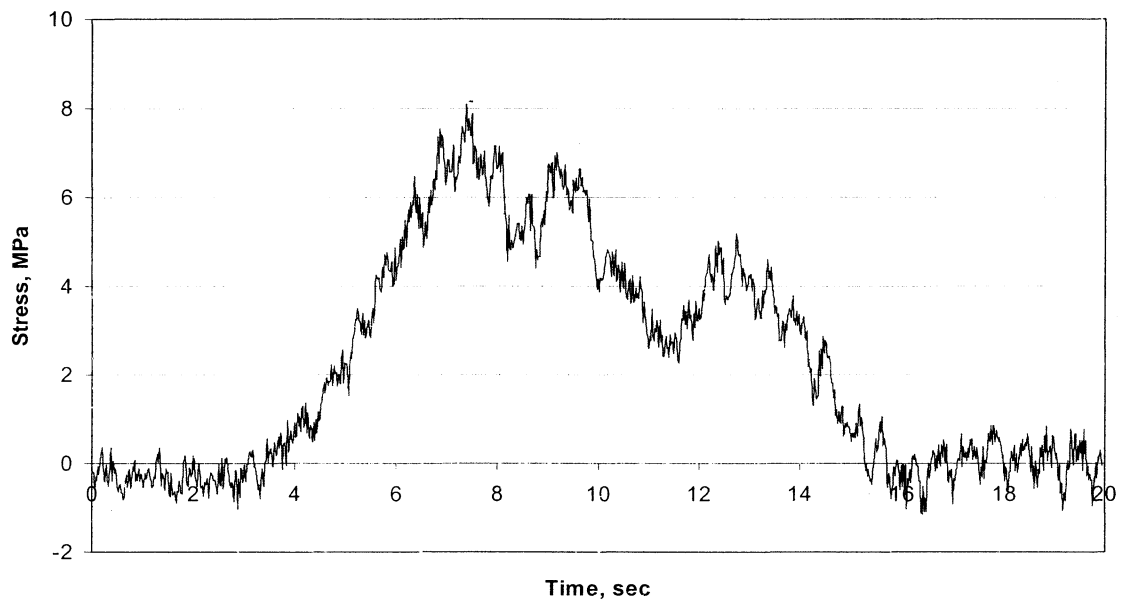
A

**Test 2; Diagonal of West Truss**



B

Test 2; Upper Chord of West Truss



C

Figure 13: Time Histories of the Response During Test 2

### **TEST 3 RESULTS**

The goal of the third test was to load one of the main trusses directly with a line of trucks. However, the trucks were unable to follow any closer than 30.5 meters, resulting in the inability to achieve the desired effect. Instead, the truss responded to the loading of only one truck at a time. The effect of one truck on the truss is barely discernible, and the resulting stress ranges were less than 3.5 MPa. As a result of these low stress ranges, this test will not be discussed further.

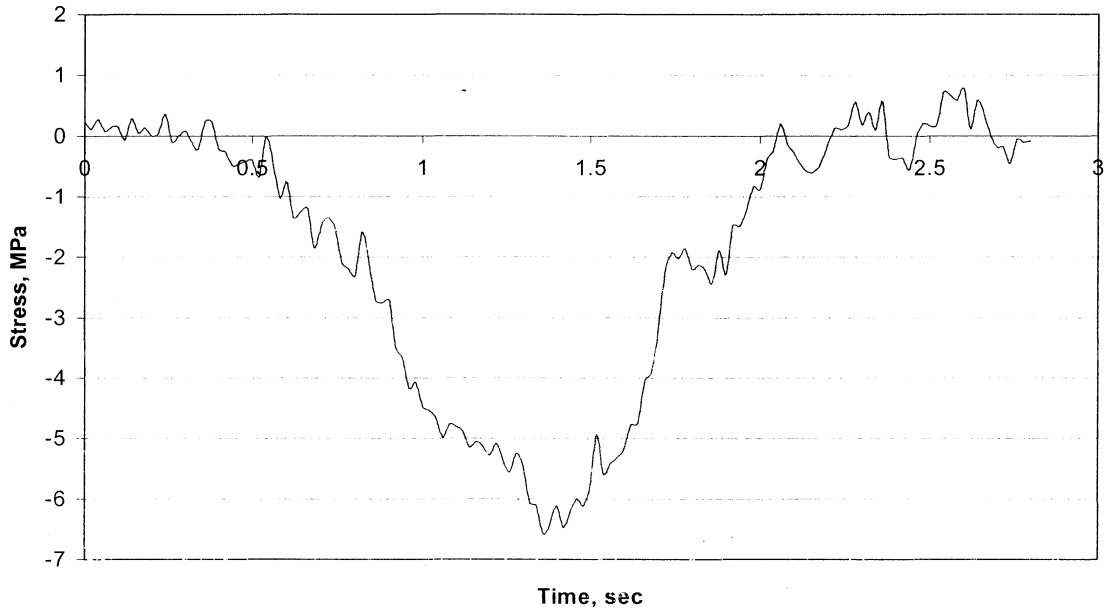
### **TEST 4 RESULTS**

This test was another attempt at creating large stress ranges in the floor truss, as well as a means to determine how the load was distributed across the width of the bridge. The maximum stress range for this test occurred in the lower chord of the floor truss and measured 14 MPa. The diagonal and upper chord of the floor truss experienced a maximum stress range of 9 and 7 MPa, respectively. The maximum stress range in the main truss was in the lower chord of the west truss and measured 8 MPa. The maximum stress ranges in the upper chord and diagonal measured 5 and 6 MPa, respectively. The time histories for all gaged members of the floor truss and west truss are shown in Figures 14a-f.

### **OPEN TRAFFIC RESULTS**

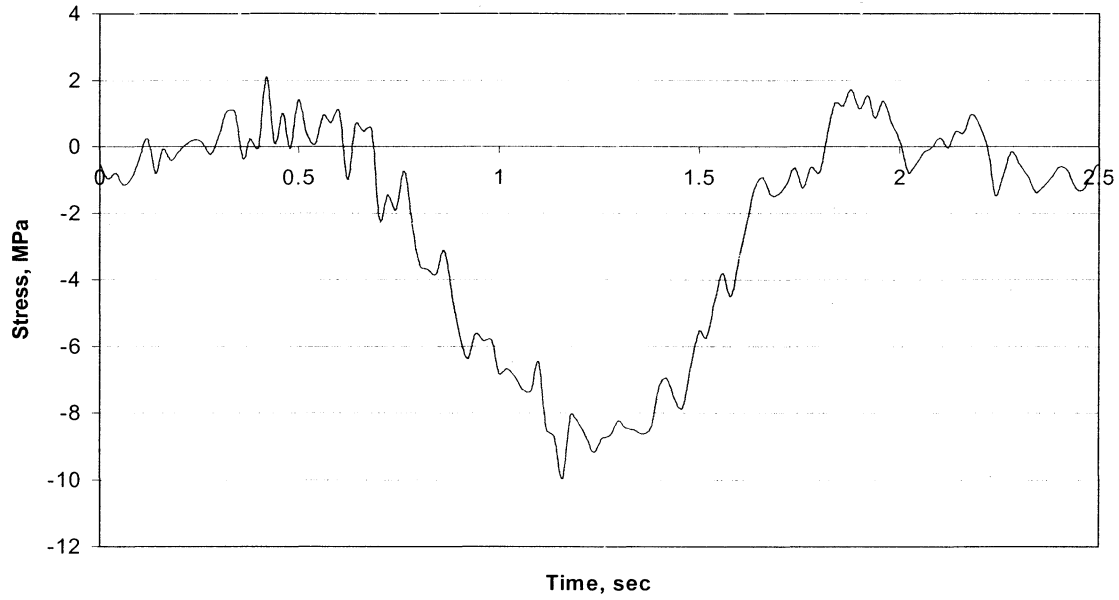
Open traffic was monitored during a four-month duration. Continuous data were collected for a limited time and during most of the time data were only recorded when triggered. During this time, the maximum stress ranges in each truss were 13 MPa in the lower chord of the east truss, 12 MPa in the lower chord of the west truss and 26 MPa in the diagonal of the floor truss.

### Test 4; Upper Chord of Floor Truss



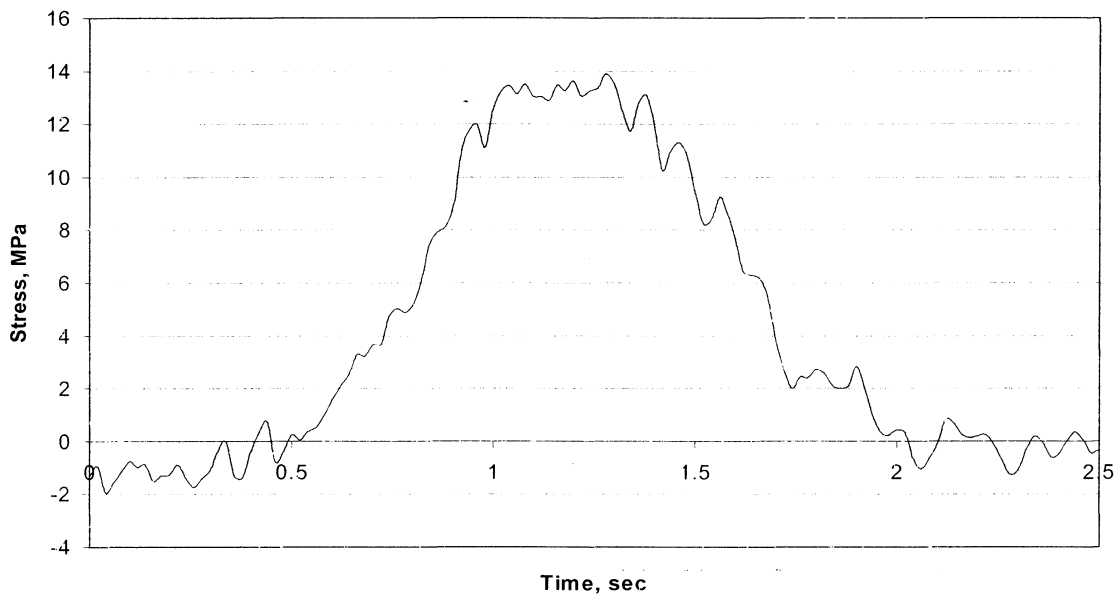
A

### Test 4; Diagonal of Floor Truss



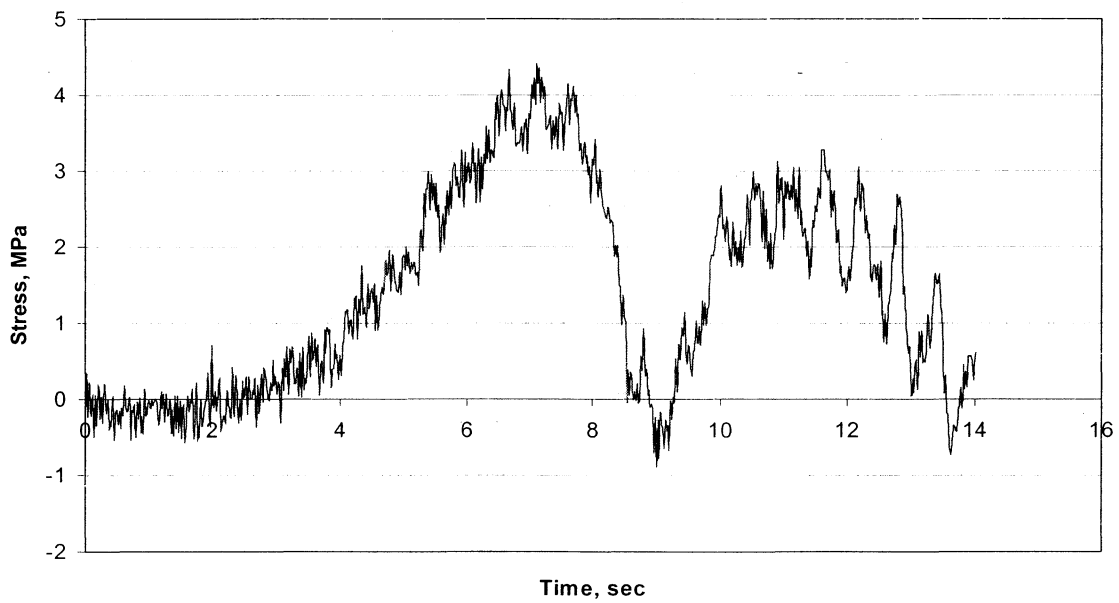
B

Test 4; Lower Chord of Floor Truss



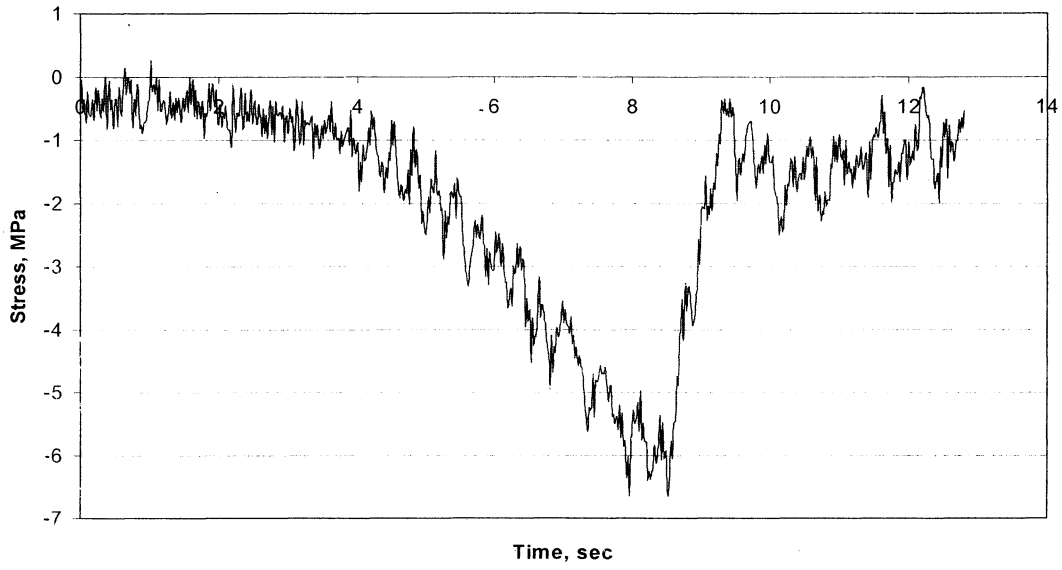
C

Test 4; Upper Chord of West Truss



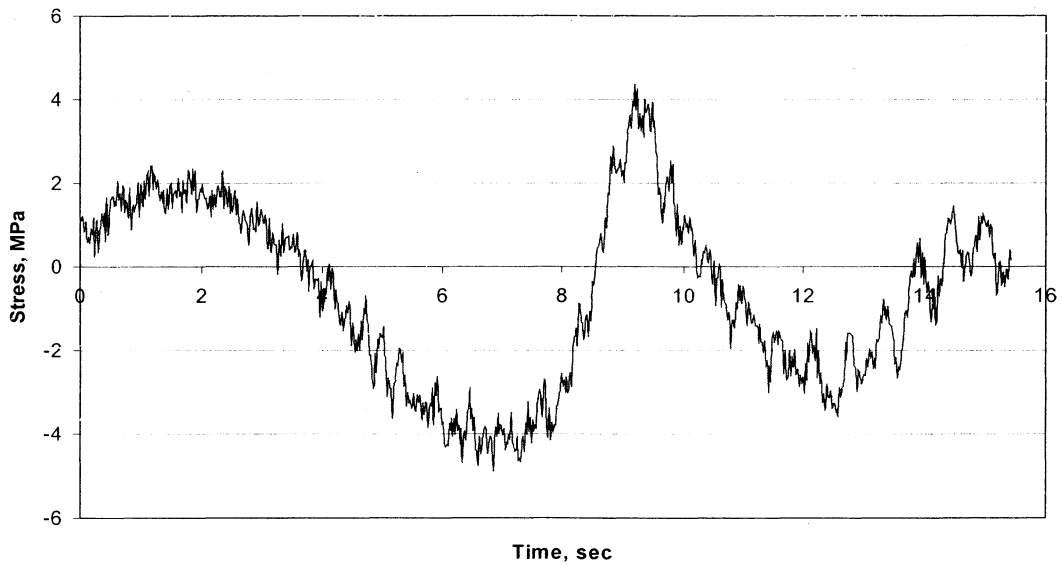
D

Test 4; Diagonal of West Truss



E

Test 4; Lower Chord of West Truss



F

Figure 14: Time Histories of the Response During Test 4

Note that these peak stress ranges are comparable to the stress ranges measured during the controlled load tests.

The largest floor truss stress history is presented in Figure 15. The diagonal member is in compression when a load is traveling in the northbound direction, directly over the gaged members, and is in tension when a load is traveling in the southbound direction. Therefore it can be assumed that this large event occurred when two large trucks, each traveling in opposite directions, passed the gaged location within seconds of each other.

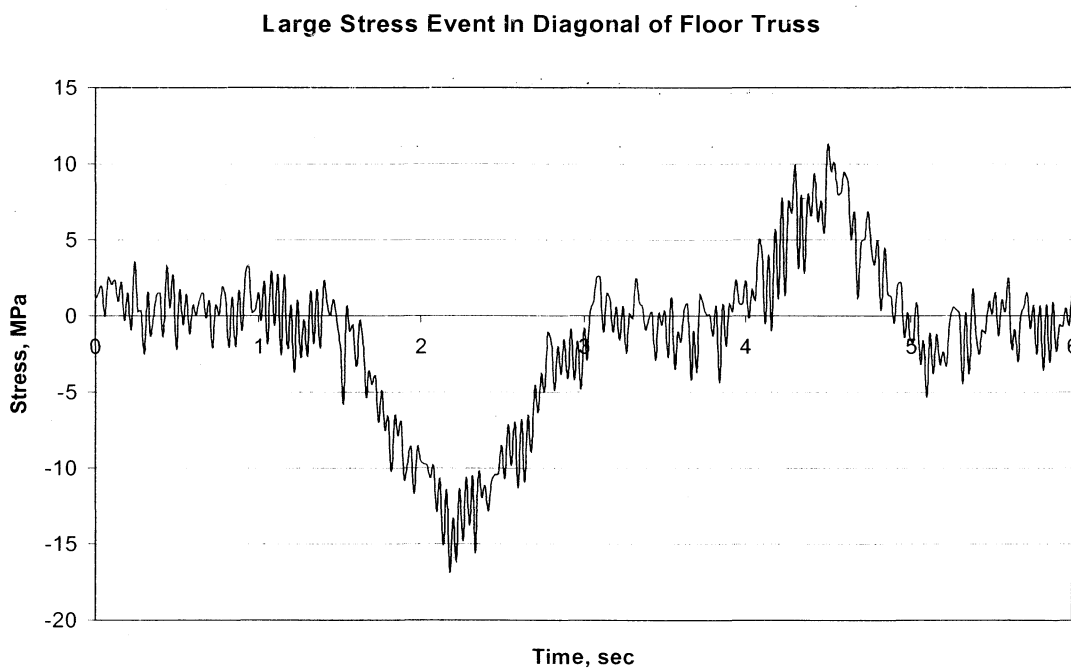


Figure 15: Largest Stress Event Recorded in Open Traffic Conditions

All data collected were imported into an Excel spreadsheet and cycles were counted using an algorithm programmed in Visual Basic in Excel. The algorithm is based on the “level-crossing” cycle counting method. This method counts a new cycle every time the stress crosses from below the mean to above a designated threshold.

To avoid counting thousands of small insignificant fluctuations as stress cycles, cycles were not counted until the stress increased above a threshold stress, which was set at 4.5 MPa, which is less than 15 percent of the smallest fatigue limit (31 MPa for Category E). The stress range associated with a cycle is the algebraic difference between the maximum peak of the stress value between incidents of crossing the cut-off stress and the minimum stress.

This method ignores the fluctuations that occur in a cycle. For example, if one were to apply this method to the main truss, the cycle in Figure 13b would be counted as one cycle with a range of 10 MPa. Note that after the peak, the stress declined to about 5.5 MPa and then increased again to about 8.75 MPa. This intermediate stress range of 3.25 MPa (from 5.5 to 8.75 MPa) is ignored. The level crossing method is the most appropriate for this type of loading as it gives a better correspondence between cycles and trucks. Since, as it turns out, none of the stress ranges exceed the thresholds for the details, the effect of ignoring the smaller intermediate stress ranges is inconsequential.

Each stress range over the cut-off stress of 4.5 MPa was tabulated. These stress ranges were sorted into discrete bins of 3.5 MPa intervals for each member in the floor truss. The

distributions of the stress range data for continuous periods of monitoring are presented in Tables 3-5.

Table 3: Stress Range Percentages During Constant Data Collection For the East Truss

Stress Range (MPa)	Upper Chord	Diagonal	Lower Chord
0-3.5	56.4	16.6	4.1
3.5-7	43.6	80.7	42.7
7-10.5	0.0	2.7	48.5
10.5-14	0.0	0.0	4.7

Table 4: Stress Range Percentages During Constant Data Collection For the West Truss

Stress Range (MPa)	Upper Chord	Diagonal	Lower Chord
0-3.5	65.0	49.4	9.1
3.5-7	35.0	49.8	78.4
7-10.5	0.0	0.8	11.9
10.5-14	0.0	0.0	0.6

Table 5: Stress Range Percentages During Constant Data Collection For the Floor Truss

Stress Range (MPa)	Upper Chord	Diagonal	Lower Chord
0-3.5	3.8	2.3	1.9
3.5-7	76.4	48.7	40.5
7-10.5	19.2	36.0	34.1
10.5-14	0.6	10.6	18.3
14-17.5	0.0	2.0	4.3
17.5-21	0.0	0.3	0.9
21-24.5	0.0	0.06	0.1
24.5-28	0.0	0.03	0.0

From the above tables it can be seen that the percentage of stress ranges in each bin for the east truss is very similar to that of the west truss, with slightly greater stress ranges in the east truss (under the northbound traffic). It is also notable that less than one in 1000 stress events in the diagonal of the floor truss exceeds 21 MPa and less than one in 3300 stress events in this member exceed 24.5 MPa. Not a single stress event recorded in any truss during constant data collection exceeded its fatigue threshold or CAFL for the details.

These histograms were then used to determine an effective stress range for each member using Equation 1. The fatigue damage caused by a given number of cycles of the effective stress range is the same as the damage caused by an equal number of the different stress ranges defined by the histograms. The effective stress ranges for the east, west and floor trusses are shown in Table 6. Again, the east truss seems to have slightly greater effective stress ranges.

Table 6: Effective Stress Ranges From Constant Data Collection

Member	East Truss	West Truss	Floor Truss
Upper Chord	4.04 MPa	3.78 MPa	6.89 MPa
Diagonal	5.14	4.31	13.91
Lower Chord	10.27	6.51	17.03

The gages in the east truss displayed excessive noise during triggered data collection and therefore are not included in the following discussion. The stress distributions displayed as percentages of all stress ranges recorded during triggered data collection are presented in Tables 7 and 8 and the effective stress ranges for each member of each truss are presented in Table 9.

Table 7: Stress Range Percentages During Triggered Data Collection For the West Truss

Stress Range (MPa)	Upper Chord	Diagonal	Lower Chord
0-3.5	58.5	38.6	30.0
3.5-7	41.4	61.0	43.2
7-10.5	0.0	0.4	26.4
10.5-14	0.0	0.0	0.4

Table 8: Stress Range Percentages During Triggered Data Collection For the Floor Truss

Stress Range (MPa)	Upper Chord	Diagonal	Lower Chord
0-3.5	13.3	36.8	3.0
3.5-7	51.1	30.9	24.5
7-10.5	34.2	25.5	55.0
10.5-14	1.4	5.5	14.6
14-17.5	0.0	1.0	2.7
17.5-21	0.0	0.2	0.3
21-24.5	0.0	0.04	0.01

Table 9: Effective Stress Ranges From Triggered Data Collection

Member	West Truss	Floor Truss
Upper Chord	3.83 MPa	6.6 MPa
Diagonal	4.53	7.06
Lower Chord	7.37	7.26

These distributions of triggered data are not directly comparable to the distributions shown in Tables 3-5, because a substantial number of the stress ranges are not recorded during the triggered-data periods. The triggering was based on large stress ranges in the lower chords of the trusses, therefore the distributions and effective stress ranges for the triggered data in the diagonal and upper chord of the main truss and floor truss show a larger percentage of smaller stress ranges. However, the peaks of the distributions look similar.

## REVERSAL AND HIGH-TENSION-STRESS MEMBER TEST RESULTS

A limited amount of continuous open-traffic data was also taken for the reversal and high-tension-stress members of the main truss. The data were reduced in the same manner as in the open traffic tests using the algorithm programmed in Visual Basic in Excel. The individual stress events were separated into bins, and the resulting percentages of all stress events in each bin are presented in Table 10.

The effective stress range members L3U4 and U4U6 are 7.9 and 5.7 MPa, respectively. The largest stress range recorded was 22 MPa in the high-tension-stress member, L3U4. The time history of this event is presented in Figure 16. The stress ranges recorded for the reversal member, U4U6, never exceeded 13 MPa.

Table 10: Stress Range Percentages During Continuous Data Collection  
for the Reversal Member (U4U6) and High-Tension-Stress Members (L3U4)

Stress Range (MPa)	L3U4	U4U6
0-3.5	5.2	1.0
3.5-7	63.3	92.4
7-10.5	21.9	6.3
10.5-14	6.9	0.3
14-17.5	2.3	0.0
17.5-21	0.1	0.0
21-24.5	0.3	0.0

### Largest Stress Event in High Tension Member L3U4

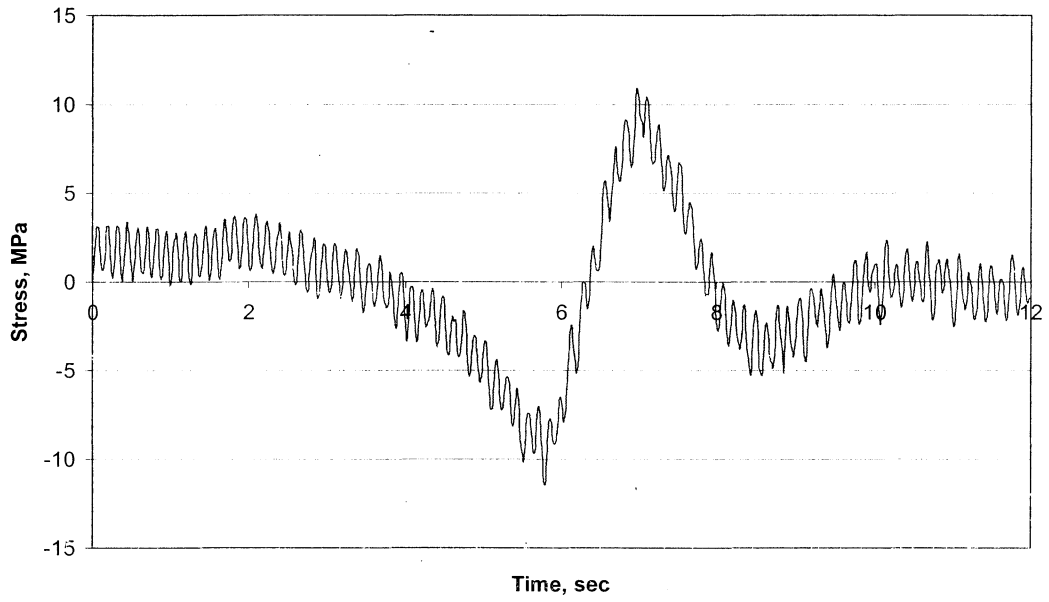


Figure 16: Largest Stress Event in High-Tension-Stress Member L3U4

## CHAPTER 6

### RESULTS OF ANALYSES

#### 2-D ANALYSIS OF MAIN TRUSS

The computer program Visual Analysis was used to model the main truss and analyze the loads applied during Tests 2 and 4. First, a two-dimensional model of the main truss was created based on the plan dimensions (Figure 17). Influence lines were then calculated for the trusses across the width of the bridge and between panel points along the length of the bridge to determine how the loads would be distributed.

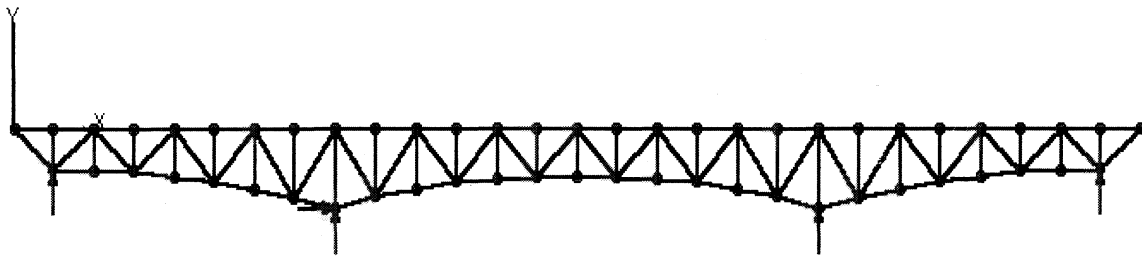


Figure 17: 2-D Visual Analysis Model of Main Truss

To apply the loads, 227 kN Mn/DOT tandem axle trucks were modeled as having only a front and rear axle spaced at 4.88 meters. We did not have measurements of each axle weight, so we assumed one third of the truck weight was placed on the front axle, and two-thirds was placed on the rear axle. This weight distribution was estimated from independent axle weigh tickets of trucks used in the study of Bridge 4654 [12].

## **Test 2**

The load distribution across the bridge deck was first checked by plotting the time histories for an east truss and west truss member during Test 2. The percentage of the west truss member stress felt by the east truss was then compared to the percentage predicted by an influence line. The data presented in Figure 18 shows that the east truss recorded 30 percent of the stress recorded in the west truss during Test 2. Calculations from a simple influence line yield a percentage of 28, suggesting good agreement between theoretical and actual distribution.

To analyze the results of Test 2, trucks were centered in their lanes as shown in Figure 11b. By measuring the time between peaks in the stress history and estimating the trucks travel speed at 88 kph, it was determined that the following distances for the three rows of trucks was 30.5 and 39.6 meters. Loads were applied to the model with appropriate distances between them and were moved across the length of the bridge.

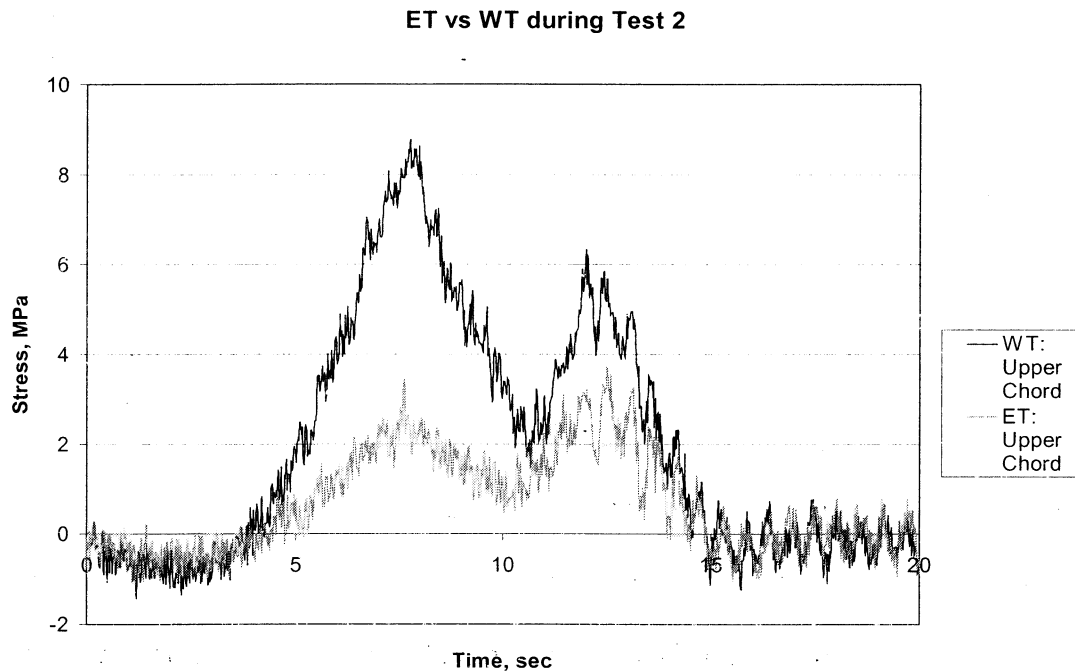
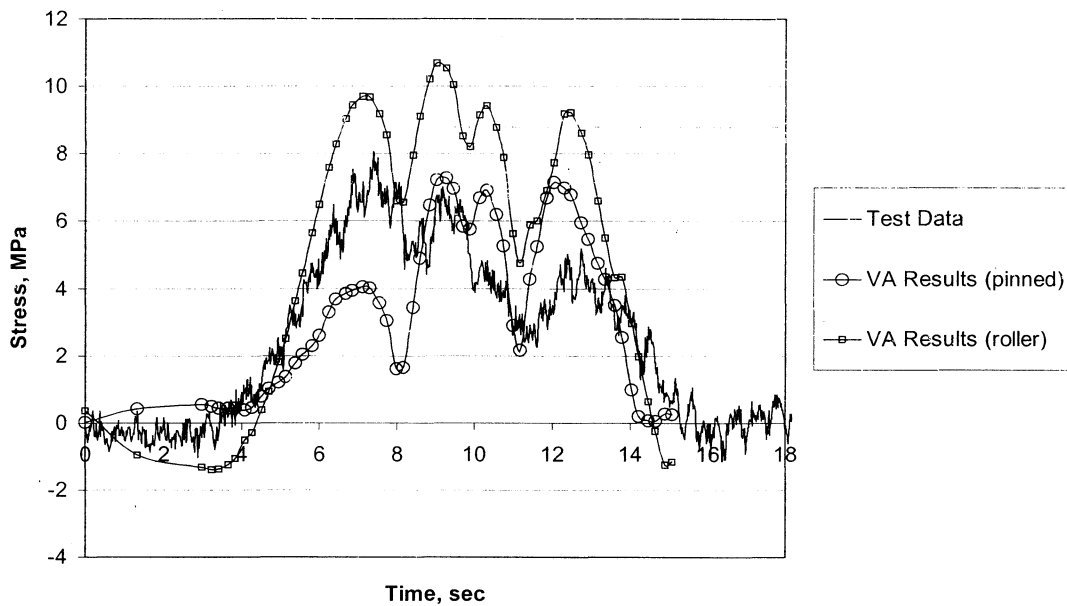


Figure 18: Distribution of Load Across the Bridge Deck

As discussed in Chapter 2, the disparity between actual and predicted stress ranges can often be attributed to unexpected partial end fixity at abutments. Therefore, the bridge was first modeled as designed with three of the four bearings defined as roller connections, allowing displacement along the length of the bridge. A second model was then made where all bearings were pin connections, restricting any longitudinal displacement. The effect of restraining the movement from the live load is to make the truss behave more like an arch, which increases the compressive force in the lower diagonal but reduces the forces in the diagonal and upper chord.

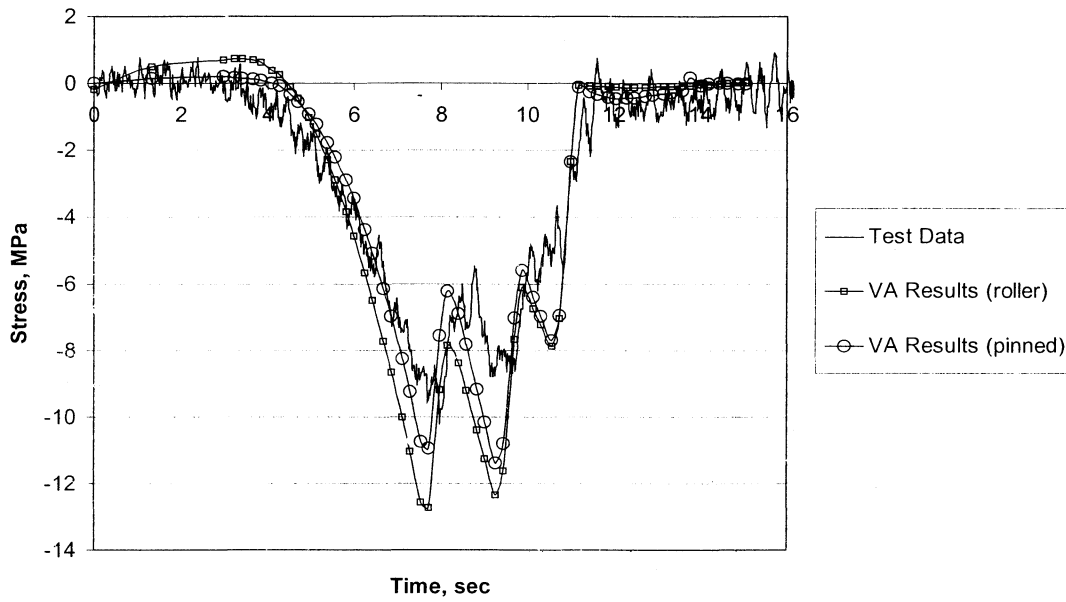
From the plots of the analytical results versus the actual time histories for Test 2 in Figure 19a-c, one can see that for the upper and lower chord, the actual stress lies somewhere in between the roller support and pinned support analyses. This is to be expected, as it is unlikely that the support neither totally restrains movement nor is completely free.

Test Data vs VA Results For Test 2; Upper Chord of West Truss



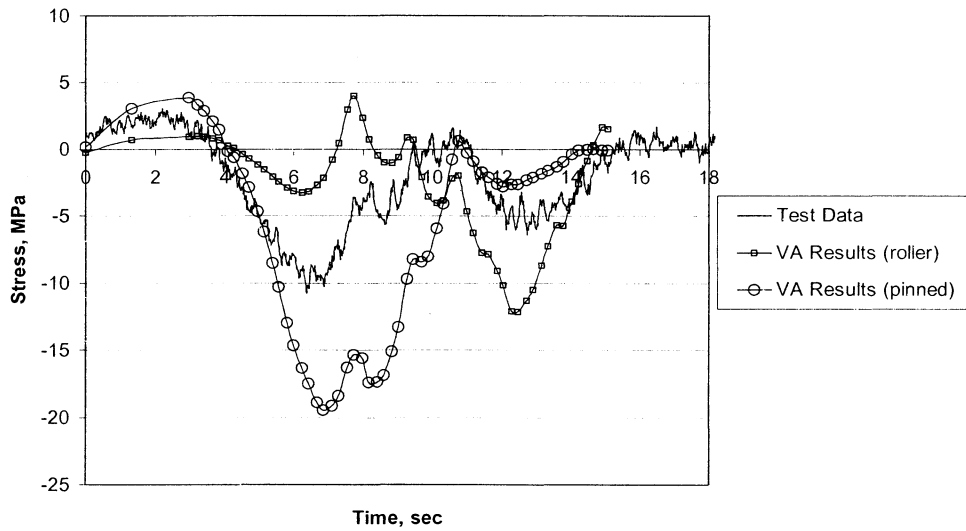
A

Test Data vs VA Results For Test 2; Diagonal of West Truss



B

Test Data vs VA Results For Test 2; Lower Chord of West Truss



C

Figure 19: Comparison of 2-D Analysis and Test Data for Main Truss in Test 2

The resulting ratios of actual to predicted stress ranges for each member are presented in Table 11. The agreement of the upper chord and diagonal members is better with the pinned model. For the lower chord, the roller model gives a stress range that is in better agreement with the actual measured stress range. However, Figure 19c shows that the shape of the stress history is much closer to the pinned model.

Table 11: Ratio of Actual to Predicted Stresses in Main Truss for 2-D Analysis of Test 2

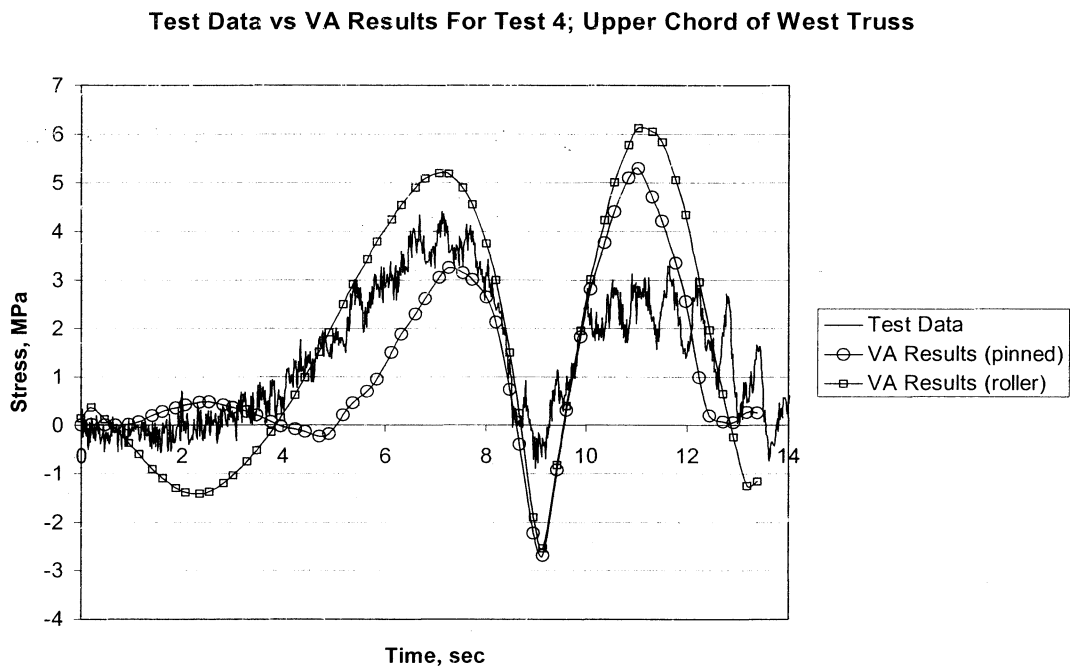
Member	Roller Bearings	Pinned Bearings
Upper Chord	68%	113%
Diagonal	58%	82%
Lower Chord	78%	53%

The upper chord recorded a stress range of 8 MPa during Test 2. Comparatively, analysis predicted stress ranges of 11.7 and 7.1 MPa for roller and pinned bearings, respectively. Likewise for the diagonal, the recorded stress range was 9.5 MPa and predicted stress ranges were 16.4 and 11.6 MPa for roller and pinned bearings. Lastly, for the lower chord, the recorded stress range was 12.5 MPa while the predicted stress ranges were 16.1 and 23.4 for roller and pinned bearings.

In conjunction with the unknown amount of fixity at the bearings, many other assumptions made in analysis could have led to the variance between actual and predicted stress ranges.

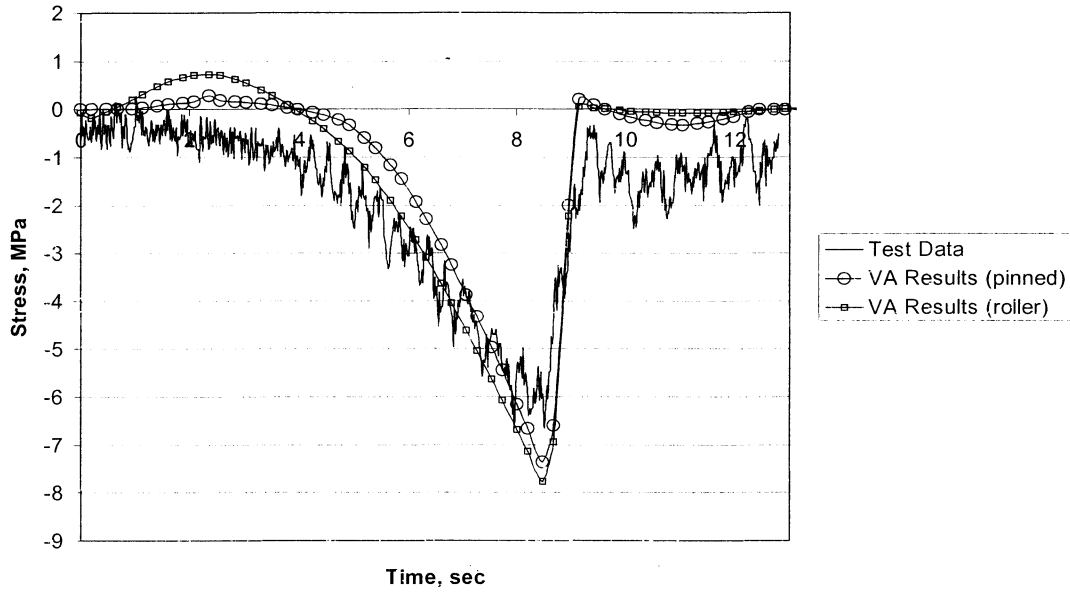
## Test 4

Test 4 was analyzed with the same model used to analyze Test 2. The bridge pier supports were also again modeled using roller bearings and pinned bearings. Influence lines were used to determine how loads were to be applied to the model. It was assumed that the trucks were centered in each lane and aligned as shown in Figure 11d. The results of the analyses are shown in Figures 20a-c.



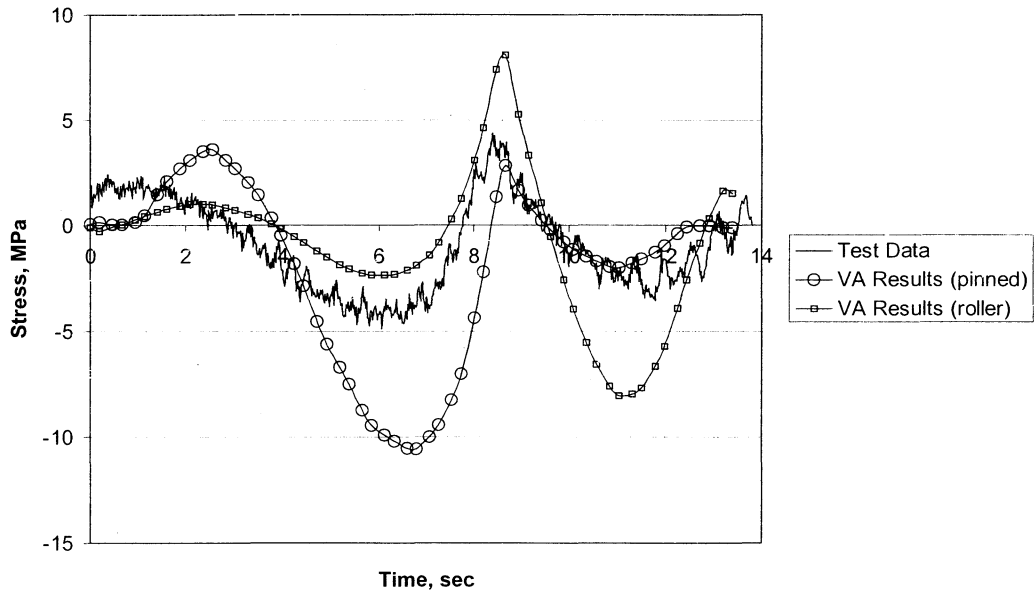
A

Test Data vs VA Results For Test 4; Diagonal of West Truss



B

Test Data vs VA Results for Test 4; Lower Chord of West Truss



C

Figure 20: Comparison of 2-D Analysis and Test Data for Main Truss in Test 4

The results of the analyses again show that for the upper and lower chords, the actual response fall between the predictions for roller and pinned bearings. The predicted response of the diagonal also shows that the bearing type has little effect on the internal stress. This is in good agreement with the analyses for Test 2.

During Test 4 the upper chord of the main truss recorded a stress range of 5 MPa. Comparatively, analysis predicted stress ranges of 9 and 8 MPa for roller and pinned bearings, respectively. The diagonal recorded a stress range of 6 MPa and predicted stress ranges were 9 and 8 MPa for roller and pinned bearings. Finally, the lower chord recorded a stress range of 8 MPa while the predicted stress ranges were 16 and 14 for roller and pinned bearings. The resulting ratios of actual to predicted stress ranges for each member are presented in Table 12.

Table 12: Ratio of Actual to Predicted Stresses in Main Truss for 2-D Analysis of Test 4

Member	Roller Bearings	Pinned Bearings
Upper Chord	58%	63%
Diagonal	71%	78%
Lower Chord	50%	56%

The ratios of actual to predicted stresses are much more consistent for Test 4 than for Test 2. This is most likely due to the fact that the formation for Test 4 was easier to maintain than the Test 2 formation. Here the analyses with pinned bearings were consistently more accurate than that with roller bearings.

### 3-D ANALYSIS OF TRUSS SYSTEM

As discussed in Chapter 2, unexpected composite action between the deck and stringers in bridges often occurs, resulting in different values for actual and predicted stresses. To try and refine the analyses conducted on the main truss, a three-dimensional model incorporating the concrete deck was constructed using SAP2000. For simplicity, the deck was modeled as a beam running transverse to the roadway with a thickness of 16.5 cm (the actual thickness of the deck) and a width of 8.0 m, the effective width given the span length as defined by ACI [23]. Instead of sitting atop stringers, short, stiff stub columns were used. W27x539 shapes were selected for the columns for maximum stiffness and placed at the nodes of the upper chords of the floor truss (Figure 21).

Since the 3-D analysis is meant to refine the current analyses, it was only applied to Test 4 as it was the most accurate and consistent under 2-D analysis. The bearings were again modeled as both roller and pinned supports. The results of the analyses are presented in Figure 22a-c.

The stress ranges were more accurate for the upper chord and diagonal, but the stress ranges in the lower chord ranged from worse when the bearings were modeled as rollers to only slightly better with pinned bearings. In the upper chord, the predicted stresses for roller and pinned bearings were 5.2 and 5.4 MPa, respectively, compared to an actual stress range of 5 MPa. The diagonal recorded a stress range of 6 MPa while the analyses predicted 11.4 and 11.7 MPa for the roller and pinned bearings. Lastly, the lower chord recorded a stress range of 8 MPa and analyses predicted 16 and 11.7 MPa for the roller and pinned bearings. The ratio of actual to predicted stress ranges is presented in Table 13.

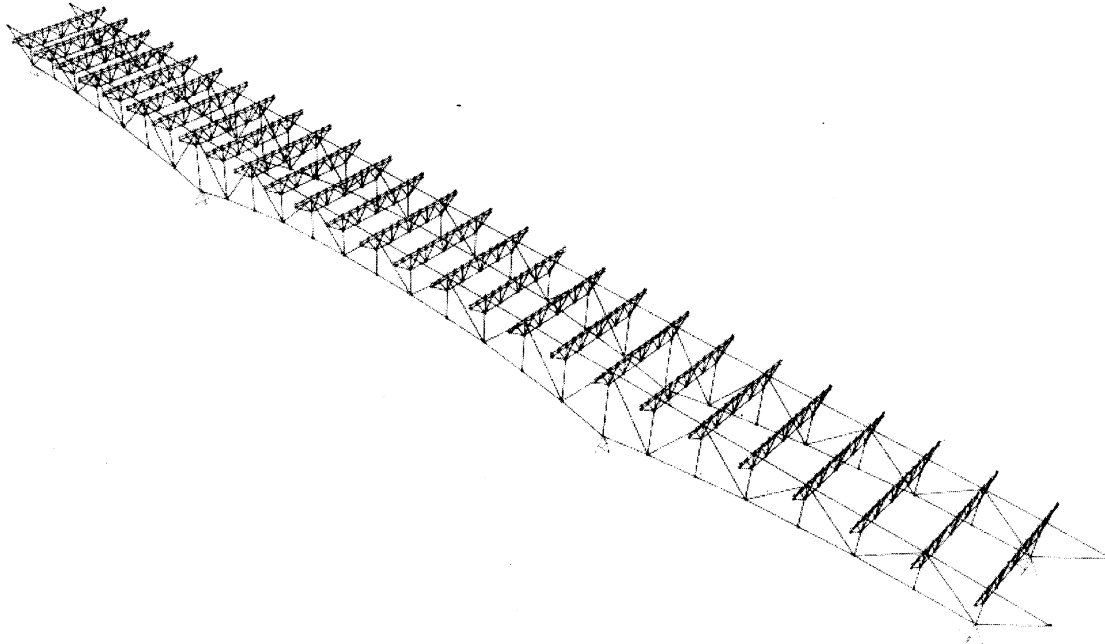
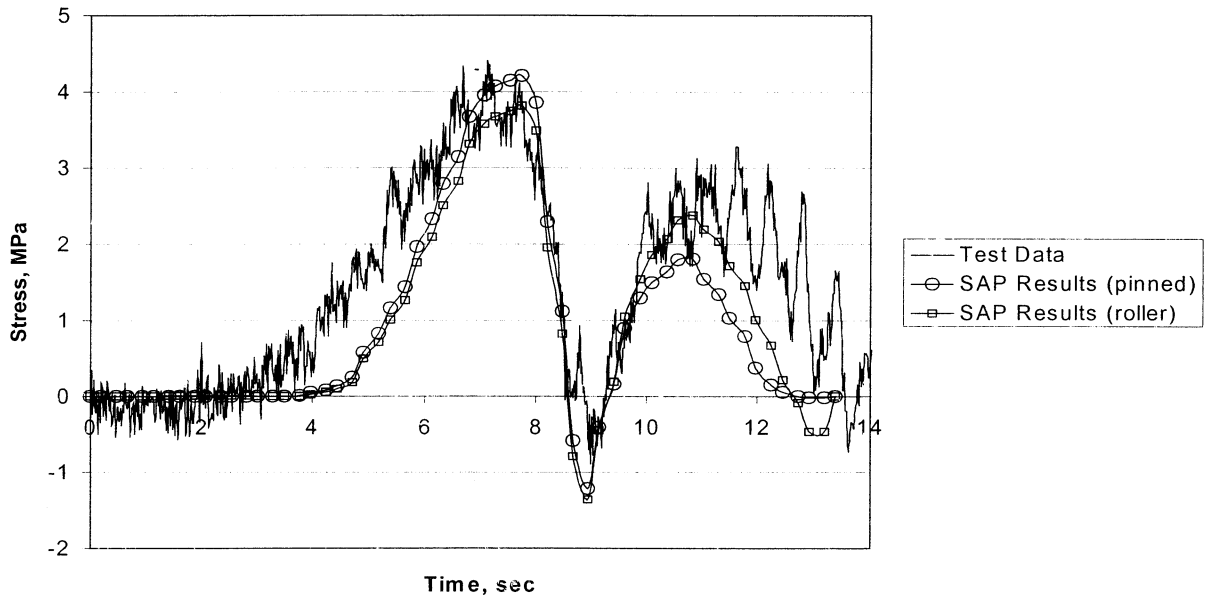


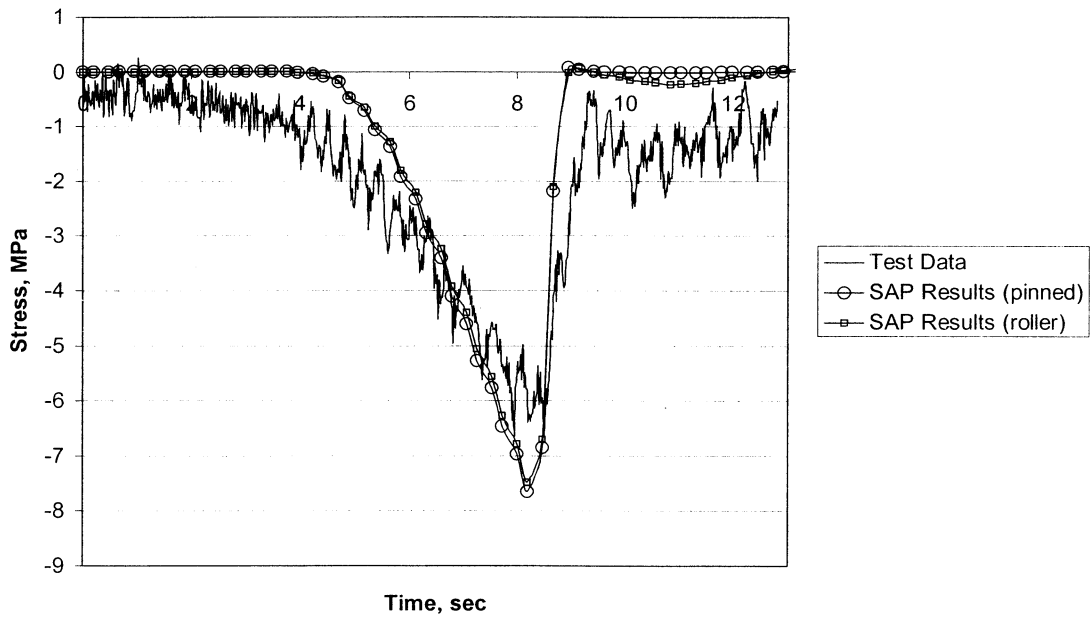
Figure 21: 3-D SAP2000 Model

Test Data vs SAP Results For Test 4; Upper Chord of West Truss



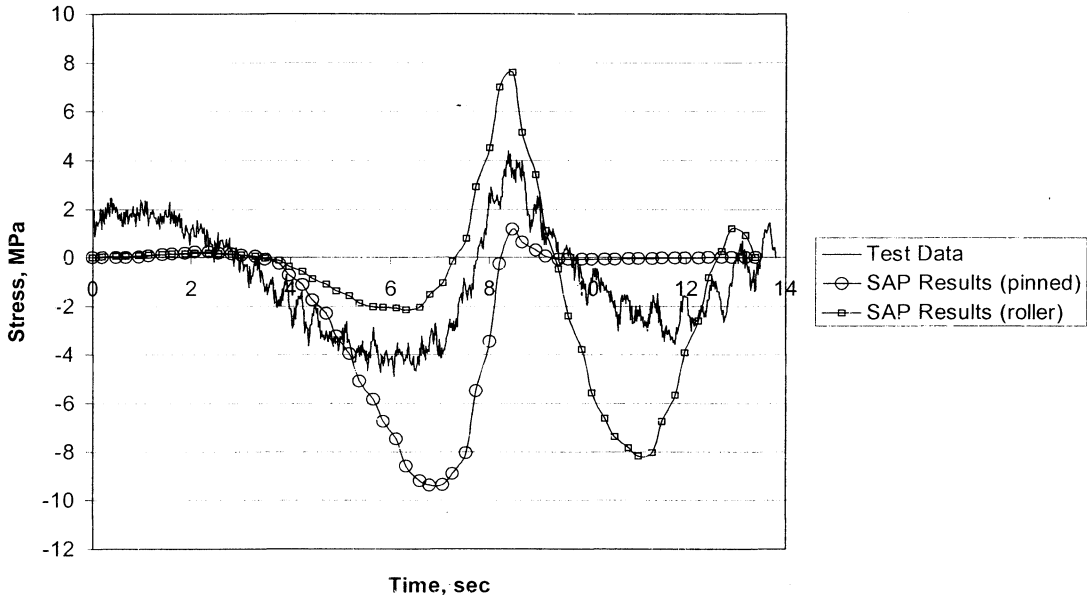
A

Test Data vs SAP Results For Test 4; Diagonal of West Truss



B

Test Data vs SAP Results for Test 4; Lower Chord of West Truss



C

Figure 22: Comparison of 3-D Analysis and Test Data for Main Truss in Test 4

Table 13: Ratio of Actual to Predicted Stresses in Main Truss for 3-D Analysis of Test 4

Member	Roller Bearings	Pinned Bearings
Upper Chord	96%	93%
Diagonal	80%	78%
Lower Chord	50%	75%

The type of bearing used in analysis had minor effects on the results for the upper chord and diagonal, however, the predicted response of the lower chord changed drastically. The total stress range of the lower chord was 75 percent of the actual stress range using pinned bearings in the model, however, once the row of trucks passed over the pier to the south of the lower chord, the predicted stresses went to zero. When the bearing to the south of the lower chord is pinned, it prevents any horizontal load from being transferred to the lower chord. The fact that the lower chord did feel load after the trucks passed the bearing to the south of it again confirms the assumption that the bearings are neither fully restrained nor free to displace.

The ratio of actual to predicted stresses in the diagonal were the same as in the 2-D analysis when pinned bearings were used, however, the ratio increased by nine percent from the 2-D analysis when roller bearings were used. Still, the predicted response for the diagonal changed the least under 3-D analysis. This follows that there are not any alternative load paths for the flow of shear force in the truss regardless of changes made at the upper or lower chords.

The upper chord predictions changed the most from the 2-D to 3-D analysis. By adding the concrete deck, the effective depth of the truss was slightly increased thus lowering the predicted stresses in the upper chord. This confirms that the concrete deck contributes a significant amount of stiffness to the truss system and should be included in any model of the bridge.

## POSSIBLE PROBLEM MEMBERS AND REMAINING LIFE IN MAIN TRUSS

Based on the completed analysis and recorded stress ranges in open traffic conditions, members that may exceed the fatigue limit can be identified. The largest stresses recorded in testing occurred during Test 2. The results from a Visual Analysis model using this loading and both pinned and roller bearings are shown in Table 14.

Table 14: Predicted Stresses Exceeding Fatigue Limit During Test 2

Member	Roller Bearings	Pinned Bearings
U2L3	54 MPa	42 MPa
L3U4	49	47
U4U6	56	40

When the roller bearings are assumed, the analysis predicts that members U2L3, L3U4, and U4U6 could experience stress ranges slightly larger than the 48 MPa CAFL for the Category D details (the short clips on the diaphragms). However, when the bearings are assumed pinned, which was shown to be the more accurate assumption, the predicted stress ranges do not exceed the CAFL. Even with the pinned assumption, however, the analysis still over-predicts the stress ranges significantly. Therefore the actual stress ranges due to this loading would be even less than the stress ranges in Table 14.

The first two of these members are diagonals while the last is an upper chord. The ratio of actual to predicted stresses for diagonals and upper chords was consistently between 58 and 78 percent for the 2-D analysis of Test 4. If the largest ratio were applied to the predicted stress ranges in Table 14, the resulting stress ranges would all fall well below the CAFL (Table 15). Therefore,

all stress ranges for all members in the main truss fall below the fatigue limit for a Category D detail and remaining life for this structure is infinite.

Table 15: Corrected Predicted Stresses For Problem Members During Test 2

Member	Roller Bearings	Pinned Bearings
U2L3	42.1 MPa	32.8 MPa
L3U4	38.2	36.7
U4U6	43.7	31.2

## 2-D ANALYSIS OF FLOOR TRUSS

Visual Analysis was also used to create a two-dimensional model of the floor truss to analyze Tests 1 and 4 (Figure 23). A concrete deck was incorporated into the model to account for added strength from unexpected composite action. As in the 3-D analysis, the deck was modeled as a 16.5 cm by .8 m beam resting atop stiff stub W27x539 columns.

### Test 1

To get analytical results for the first test, the front axle of a truck was assumed to be 4.57 meters away from the rear axle of the truck directly in front of it. An influence line for the floor truss showed that the load on the truss would be largest when the rear axle of the center truck was directly on the truss. For simplicity, a single load for each axle was applied at the center of each interior lane. The maximum stress range during this test occurred in the lower chord and measured 28 MPa. The analysis yielded a maximum stress for the same member of 36.7 MPa, yielding an actual to predicted stress range ratio of 76 percent. If the distance between the front and rear axles was reduced to 3.05 meters, the analysis yielded a maximum stress in the lower chord of 42.8 MPa, a ratio of 65 percent.

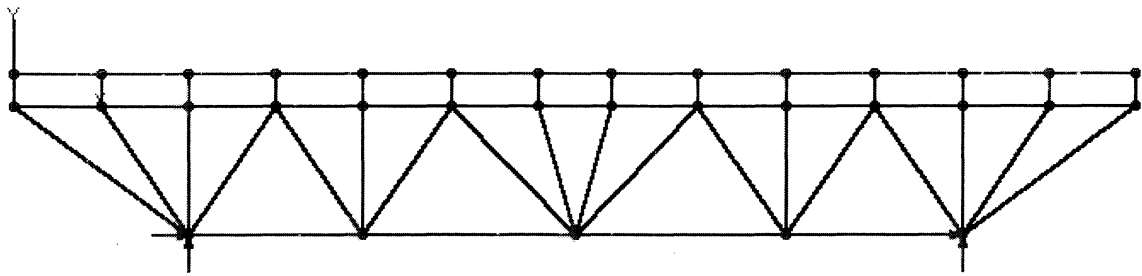
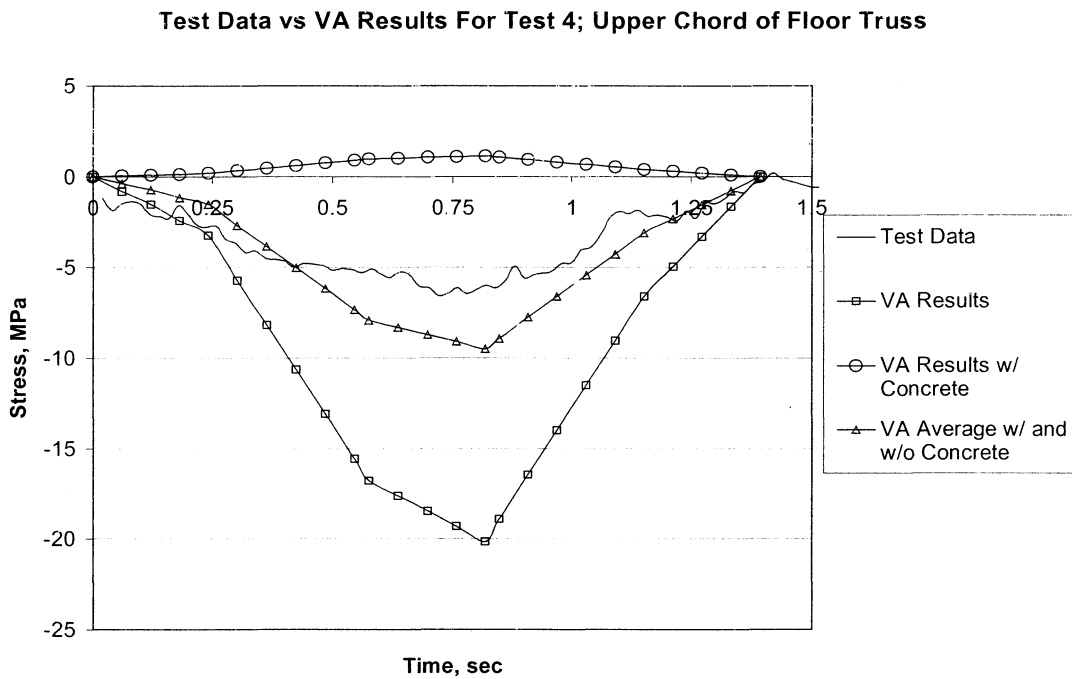


Figure 23: 2-D Visual Analysis Model of Floor Truss with Concrete Deck

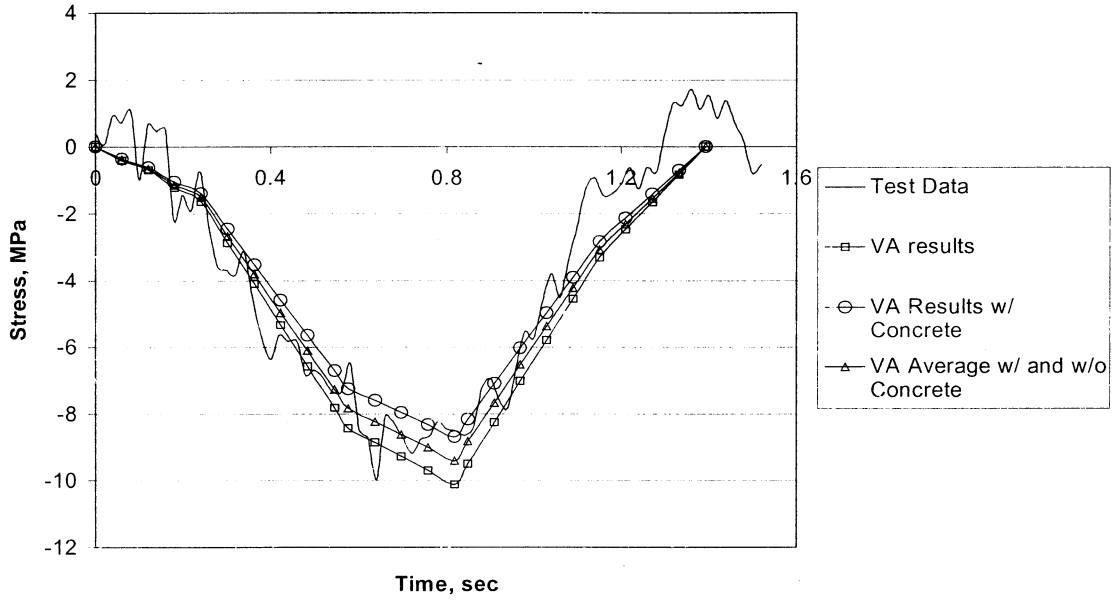
## Test 4

Analyses of the floor truss results for the fourth test were done in much the same way. Truck loads were applied to an influence line, which was used to determine the load distribution between neighboring floor trusses as the line of trucks moved across the bridge. Analysis was done with and without the concrete deck in place. Later, these results were averaged. The time histories for each member of the floor truss versus the analysis results are shown in Figures 24a-c.



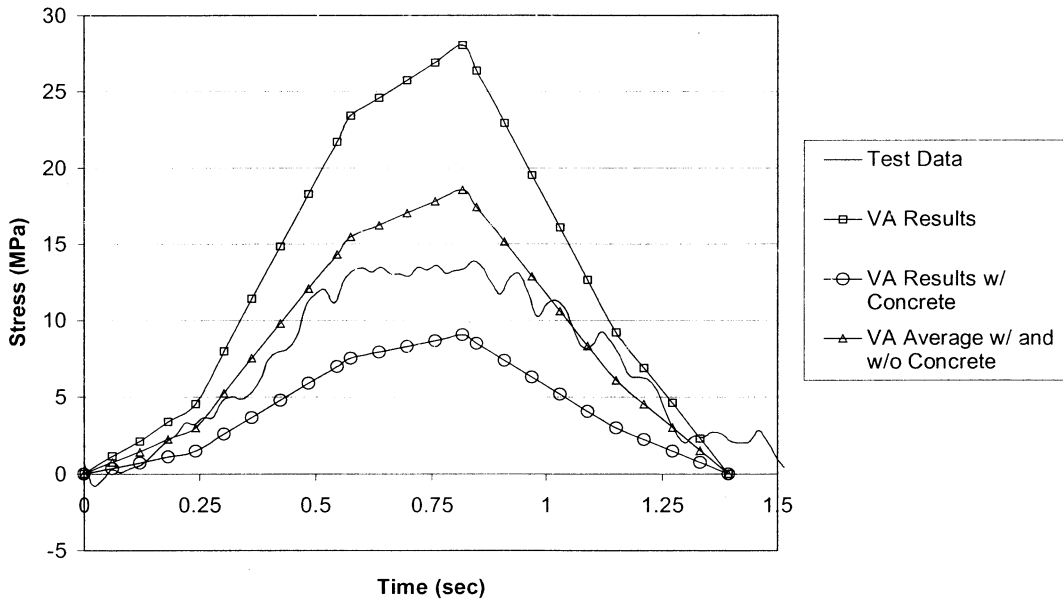
A

Test Data vs VA Results For Test 4; Diagonal of Floor Truss



B

Test Data vs VA Results For Test 4; Lower Chord of Floor Truss



C

Figure 24: Comparison of 2-D Analysis and Test Data for Floor Truss in Test 4

From these figures, it can be seen that the analysis results from the upper chord and lower chord without the concrete deck in place are much higher than the recorded stresses. Including the deck lowers the stresses too much so the two separate predicted responses were averaged to estimate the contribution of the concrete deck. This averaged predicted response shows the best correlation to the actual response. The ratio of actual to predicted stress ranges is shown in Table 16.

Table 16: Ratio of Actual to Predicted Stresses in Floor Truss for 2-D Analysis of Test 4

Member	VA Results	VA w/ Concrete	Average
Upper Chord	33%	n/a	69.5%
Diagonal	91%	106%	98%
Lower Chord	49.5%	154.4	74.7%

The stress ranges felt in the diagonal are only slightly affected by the concrete deck. This follows the results of diagonals in the other analyses. There are no alternative load paths at the diagonals, therefore a change in supports or the addition of a concrete deck have little effect.

### **REMAINING LIFE OF THE FLOOR TRUSS**

The predicted stress ranges in the floor truss never exceed the CAFL of 31 MPa for the Category E (stiffener) detail, therefore the remaining life of the floor truss is considered to be infinite. The largest predicted stress range for Test 4 occurs in member L1U4 and is 22.2 MPa when the results of the models with and without the concrete deck are averaged. Since this member is a diagonal, one can assume that the actual stress range in the member correlated well with the predicted stress range.

## CHAPTER 7

### SUMMARY AND CONCLUSIONS

Field tests and analyses were conducted on Bridge 9340 crossing the Mississippi River just east of downtown Minneapolis. Field tests were conducted in two parts. The first part involved measuring strains while trucks of known weights crossed the bridge. The second part involved monitoring the strains and counting strain cycles under open traffic conditions over a period of several months. Results of the first part were used to calibrate two and three-dimensional numerical models. Results of the second part were used to characterize the statistical distribution of the stress ranges and estimate the remaining fatigue life. The main conclusions were:

1. Inspection of the bridge revealed Category D details on the main truss members and Category E members on the floor truss. No fatigue cracks were found by visual inspection of those members.
2. The largest stress range measured in the main truss during the controlled tests was 12.5 MPa in the lower chord, from three rows of three trucks. The analyses show that member U4U6 would have the largest stress range from this loading, 46 MPa. This is less than the fatigue threshold for the most critical details on these members, which is 48 MPa for Category D.
3. The largest stress range in the main truss during the open-traffic monitoring was 22 MPa and this was in another member, L3U4.

4. The agreement of the analyses with the measured stress ranges was best when a three-dimensional model of the whole bridge was analyzed. In both the two-dimensional and three-dimensional analyses, the agreement was best if the roller bearings at the piers were assumed to be pinned so that a horizontal reaction developed and arching action occurred.
5. The largest stress range measured in the floor truss during the controlled tests was 28 MPa in the lower chord, from three rows of trucks in the leftmost lane (closest to the center) in each direction. This is less than the fatigue threshold of 31 MPa for a Category E detail.
6. The largest stress range in the floor truss during the open-traffic monitoring was 25 MPa and this was in a diagonal.
7. Two-dimensional analyses were adequate for the floor truss. Very poor agreement with the measured results was obtained unless some composite action with the deck was assumed. Full composite action was too much, and optimal results were obtained by averaging the results from the non-composite case and the fully composite case.
8. Since the measured and calculated stress ranges were less than the fatigue threshold, it is concluded that fatigue cracking is not expected in the deck truss of this bridge.

9. Live-load stress ranges greater than the fatigue threshold can be calculated if the AASHTO lane loads are assumed. The actual measured stress ranges are far less primarily because the loading does not frequently approach this magnitude. While the lane loads are appropriate for a strength limit state (the loading could approach this magnitude a few times during the life of the bridge), only loads that occur more frequently than 0.01% of occurrences are relevant for fatigue. For this bridge with 15,000 trucks per day in each direction, only loads that occur on a daily basis are important for fatigue.

The following actions are recommended:

1. The members of the main truss with the highest stress ranges are U2L3, L3U4 and U4U6. These members should be inspected thoroughly, especially at the ends of the “clips” on the diaphragms in the tension members and at any intermittent fillet welds. These members should be inspected every two years as is presently done.
2. The lower chords and diagonals of all the floor trusses also have high stress ranges. The ends of the “fin” attachments reinforcing the splice welds are the most critical locations. Since these can be inspected easily from the catwalk, they could be inspected every 6 months.

## CHAPTER 8

### REFERENCES

1. Standard Specifications for Highway Bridges, American Association of State Highway Officials, Washington DC, 1961.
2. Fisher, J.W., Frank, K.H., Hirt, M.A., and McNamee, B.M., “Effect of Weldments on the Fatigue Strength of Steel Beams”, National Cooperative Highway Research Program Report 102, Highway Research Board, Washington, D.C., 1970.
3. Fisher, J.W., Albrecht, P.A., Yen, B.T., Klingerman D.J., and McNamee B.M., “Fatigue Strength of Steel Beams With Welded Stiffeners and Attachments,” National Cooperative Highway Research Program Report 147, Transportation Research Board, Washington, D.C., 1974.
4. Fisher, J.W., Nussbaumer, A., Keating, P.B., and Yen, B.T., “Resistance of Welded Details under Variable Amplitude Long-Life Fatigue Loading”, National Cooperative Highway Research Program Report 354, Transportation Research Board, Washington, D.C., 1993.
5. Guide Specifications for Fatigue Design of Steel Bridges, American Association of State Highway and Transportation Officials, 1<sup>st</sup> Ed., Washington, D.C., 1989.
6. Standard Specifications for Highway Bridges-LRFD, American Association of State Highway and Transportation Officials, 1<sup>st</sup> Ed. Washington DC, 1994.
7. Hall, D.H., Heins, C.P., Hyma, W.R., Kostem, C.N., Krisnamurthy, N., Lally, A, Loveall, C.L, Smith, E.A., Sweeny, R.A.P, Tartaglione, L.C., and Yoo, C.H., “State-of-the-Art Report on Redundant Bridge Systems”, Journal of Structural Engineering, Vol. 111, No. 12, December, 1985.
8. Ressler, S.J., and Daniels, J.H, “Fatigue Reliability and Redundancy in Two-Girder Steel Highway Bridges”, Advanced Technology for Large Structural Systems Report No. 92-01, January 1992.
9. Faber, M.H., Val, D.V., and Stewart, M.G., “Proof Load Testing for Bridge Assessment and Upgrading”, Engineering Structures, Vol. 22, pp 1677-1689, 2000.
10. Moses, F., Schilling, C.G., and Raju, K.S., “Fatigue Evaluation Procedures for Steel Bridges,” National Cooperative Highway Research Program Report 299, Transportation Research Board, Washington DC, 1987.
11. Zwerneman, F.J., Poynter, P.G., Abbas, M.D., Rauf, A. and Yang, J., “Fatigue Assessment of Bridge Members Based on In-Service Stresses”, Oklahoma State University, 1996.
12. Dexter, R.J., Hajjar, J.F., O’Connell, H.M., Bergson, P.M., “Fatigue Evaluation of Stillwater Bridge (Bridge 4654),” Minnesota Department of Transportation, 1998.

13. Dexter, R.J., Fisher, J.W., “The Effect of Unanticipated Structural Behavior on the Fatigue Reliability of Existing Bridge Structures”, Structural Reliability in Bridge Engineering, Frangopol, D. M. and Hearn G. eds., Proceedings of a Workshop, University of Colorado at Boulder, 2-4 October 1996, McGraw-Hill, New York, pp. 90-100, 1996.
14. Burdette, E.G. and Goodpasture, D.W., “Correlation of Bridge Load Capacity Estimates With Test Data” National Cooperative Highway Research Program Report 306, Transportation Research Board, Washington, D.C., 1988.
15. Bakht, Baidar and Jaeger, L.G., “Bridge Testing-A Surprise Every Time”, Journal of Structural Engineering, Vol. 116, No. 5, May 1990.
16. Bakht, Baidar, “Ultimate Load Test on a Slab-on-Girder Bridge”, Structural Res. Rep., SRR-88-03, Ministry of Transportation, Downsview, Ontario, Canada, 1988.
17. Hahin, C., South, J.M., Mohammadi, J., and Polepeddi, R., “Accurate and Rapid Determination of Fatigue Damage in Steel Bridges”, Journal of Structural Engineering, Vol. 119, No. 1, January 1993.
18. Miner, M.A., “Cumulative Damage in Fatigue”, Journal of Applied Mechanics, 12, A-159, 1945.
19. Dexter, R.J. and Fisher J.W., “Fatigue and Fracture”, Handbook of Structural Engineering, Chapter 24, Chen, W. F. ed., CRC Press LLC, New York, 1997, pp 24-1 to 24-30.
20. Dexter, R.J. and Fisher, J.W. “Fatigue and Fracture”, Handbook of Bridge Engineering, Chapter 53, Chen, W. F. ed., CRC Press LLC, New York, 1999, 24 pages.
21. Wilson, Pete, “In-Depth Fracture Critical Bridge Inspection Report Bridge #9340: I35W over the Mississippi River (Downtown Minneapolis),” Minnesota Department of Transportation, 1997.
22. Bergson, Paul, Letter to Minnesota Department of Transportation, 21 December, 1998.
23. Code Requirements for Structural Concrete, American Concrete Institute, 1995.